

This document was prepared in conjunction with work accomplished under Contract No. AT(07-2)-1 with the U.S. Department of Energy.

DISCLAIMER

This report was prepared as an account of work sponsored by an agency of the United States Government. Neither the United States Government nor any agency thereof, nor any of their employees, makes any warranty, express or implied, or assumes any legal liability or responsibility for the accuracy, completeness, or usefulness of any information, apparatus, product or process disclosed, or represents that its use would not infringe privately owned rights. Reference herein to any specific commercial product, process or service by trade name, trademark, manufacturer, or otherwise does not necessarily constitute or imply its endorsement, recommendation, or favoring by the United States Government or any agency thereof. The views and opinions of authors expressed herein do not necessarily state or reflect those of the United States Government or any agency thereof.

This report has been reproduced directly from the best available copy.

Available for sale to the public, in paper, from: U.S. Department of Commerce, National Technical Information Service, 5285 Port Royal Road, Springfield, VA 22161
phone: (800) 553-6847
fax: (703) 605-6900
email: orders@ntis.fedworld.gov
online ordering: <http://www.ntis.gov/help/index.asp>

Available electronically at <http://www.osti.gov/bridge>

Available for a processing fee to U.S. Department of Energy and its contractors, in paper, from: U.S. Department of Energy, Office of Scientific and Technical Information, P.O. Box 62, Oak Ridge, TN 37831-0062
phone: (865)576-8401
fax: (865)576-5728
email: reports@adonis.osti.gov

~~SECRET~~

UNCLASSIFIED

~~This document consists of
45 pages. No. 24 of
25 copies, Series A.~~

RECORDS ADMINISTRATION



AYJN

DISTRIBUTION

- | | |
|--|------------------------|
| 1. M. H. Wahl - Wilm. | 12. F. E. Kruesi |
| 2. J. W. Croach -
A. A. Johnson - Wilm. | C. H. Ice - SRL |
| 3. D. F. Babcock | 13. G. Dessauer |
| 4. L. W. Fox - SRP | 14. P. L. Roggenkamp |
| 5. O. A. Towler | 15. D. E. Hostetler |
| 6. J. R. Hilley | 16. J. A. Smith |
| 7. L. A. Heinrich | 17. W. E. Graves |
| 8. W. B. Daspit | 18. V. D. Vandervelde |
| 9. R. F. Anderson | 19. E. J. Hennelly |
| 10. F. D. Benton | 20. C. E. Bailey |
| 11. A. B. Thomas | 21. J. P. Church |
| | 22. D. Randall |
| | 23. 706-C File |
| | 24. TIS File |
| | 25. Vital Records File |

TIS FILE
RECORD COPY

Classification Cancelled

BEST AVAILABLE COPY
January 19, 1989

By Authority of

RS Hill 4/8/88
Name Date

MEMORANDUM

TO: P. L. ROGGENKAMP

FROM: DUNCAN RANDALL DR

CLASSIFICATION REVIEW FOR
DECLASSIFICATION BUT LEFT
UNCHANGED

By: RE Trilled
Date: 12/12/73
U. S. AEC Division of Classification

CG115.2

XENON OSCILLATIONS IN MARK XIIIA-50

INTRODUCTION

Spatial power oscillations can occur in a sufficiently large reactor even though it is operated at constant total power. Resultant local increases in temperature can, if uncontrolled, cause local boiling and even fuel element failure. Fortunately, these oscillations occur with periods usually of the order of several hours, so that ample time is available in which to damp out these regional perturbations by local control rod movement. The oscillations are caused by changes in the spatial distribution of Xenon-135 and require a perturbation of the power distribution to be initiated.

RESTRICTED DATA

THIS DOCUMENT CONTAINS RESTRICTED DATA AS DEFINED IN THE ATOMIC ENERGY ACT OF 1954. ITS TRANSMITTAL OR THE DISCLOSURE OF ITS CONTENTS IN ANY MANNER TO AN UNAUTHORIZED PERSON IS PROHIBITED.

GROUP 1 - EXCLUDED FROM AUTOMATIC DOWNGRADING AND DECLASSIFICATION

UNCLASSIFIED

~~SECRET~~

UNCLASSIFIED

~~SECRET~~

-2-

P. L. ROGGENKAMP

DPST-68-206

The modal analysis technique developed at SRL^(1,2) permits calculation of the threshold flux level at which sustained (i.e., constant amplitude) spatial xenon and flux oscillations can occur, and calculation of the oscillation period at this threshold level. The added buckling required to excite the first axial or radial flux harmonic is computed, taking into account the temperature coefficient and any degree of central flattening of the fundamental flux shape. The program also permits evaluation of periods of non-steady oscillations at any desired flux levels, whether or not a threshold flux exists.

During the study of the Mark XIIIA-50 lattice, it was necessary to revise the SOS-I code in order to calculate both the lower and the upper flux thresholds which appear when the temperature coefficient is negative. The current code, XEN01747, includes these revisions and features more flexible problem input.

SUMMARY

It is concluded that:

1. The Mark XIIIA-50 load is susceptible to both axial and radial xenon oscillations.
2. Radial oscillations are more likely than axial oscillations because of the generally lower threshold fluxes associated with radial oscillations for this load.
3. Axial oscillations are possible at the start but not the end of the cycle. At the start of the cycle, when $M^2 = 260 \text{ cm}^2$, the temperature coefficient $\alpha_T = -1.63 \times 10^{-17} \text{ k/unit flux}$, and flux flattening = 80% (possibly), the lower flux = $5.36 \times 10^{13} \text{ n/cm}^2 \cdot \text{sec.}$; since this is lower than the initial average operating flux $2.05 \times 10^{14} \text{ n/cm}^2 \cdot \text{sec.}$, non-decaying xenon oscillations are possible. An upper threshold flux also exists, at $7.84 \times 10^{14} \text{ n/cm}^2 \cdot \text{sec.}$; if the actual flux exceeded this value, which it does not, then any flux tilt perturbations would die out spontaneously. At the end of the cycle, when $M^2 = 317 \text{ cm}^2$, α_T is unchanged and the flux is virtually unflattened, no flux threshold exists, so that sustained flux tilt oscillations are impossible.
4. Radial oscillations are possible at both the start and the end of the cycle. At the start of the cycle, when $M^2 = 260 \text{ cm}^2$, $\alpha_T = -2.50 \times 10^{-17} \text{ k/unit flux}$, and flux flattening = 60%, the lower threshold flux = $5.03 \times 10^{13} \text{ n/cm}^2 \cdot \text{sec.}$ and the upper threshold flux = $5.26 \times 10^{14} \text{ n/cm}^2 \cdot \text{sec.}$ Since the initial average operating flux lies between these thresholds, growing flux tilt oscillations are possible. At the end of the cycle, when $M^2 =$

~~SECRET~~

UNCLASSIFIED

UNCLASSIFIED

~~SECRET~~

-3-

P. L. ROGGENKAMP

DPST-68-206

317 cm^2 ., and both α_T and the flux flattening are unchanged, the lower flux threshold has risen (i.e., the reactor has become more stable) to 1.07×10^{14} $\text{n/cm}^2\text{.sec.}$ and the upper flux threshold has dropped to 2.87×10^{14} $\text{n/cm}^2\text{.sec.}$ Meanwhile the average operating flux has risen to 3.35×10^{14} $\text{n/cm}^2\text{.sec.}$, just above the upper flux threshold, so that the reactor is now stable to xenon oscillations at full power but not during power ascension or reduced power levels.

5. The calculated oscillation period agreed well with the observed period for a reported radial oscillation at 40% of full power. For $\alpha_T = -2.50 \times 10^{-17}$ k/unit flux, the calculated period = 20.2 hours; the observed period was 20 hours.
6. In general,
 - (a) an increased M^2 raises a single or lower threshold, so that the Mark XIIA-50 load is more vulnerable to xenon oscillations at the start of the cycle;
 - (b) a negative temperature coefficient produces a pair (if any) of flux thresholds: if the actual flux lies between these thresholds, the oscillation will grow; if it lies above the upper threshold or below the lower threshold, the oscillation will decay;
 - (c) the flux threshold based on a zero temperature coefficient lies slightly below the lower flux threshold resulting from a negative temperature coefficient; the improved stability from a negative coefficient is, however, usually too small to prevent xenon oscillations if they are possible for a zero temperature coefficient;
 - (d) a zero or positive temperature coefficient permits only one threshold flux; a positive temperature coefficient yields a still lower threshold than does a zero temperature coefficient;
 - (e) flux flattening very strongly increases susceptibility to xenon oscillations, both radially and axially.

Oscillation periods and perturbation damping factors are plotted in Figures 8-21 vs. arbitrarily-specified flux levels at, above, and below threshold values.

Raising the input value of either the xenon cross-section or the fission cross-section/absorption cross-section ratio results in lower oscillation thresholds.

~~SECRET~~

UNCLASSIFIED

UNCLASSIFIED

A value of the fission cross-section/absorption cross-section ratio is needed as input for XEN01747. An improved method of calculating this ratio was developed to take into account the heterogeneity of the lattice and the enhancement effect.

DISCUSSIONI. Input Parameters

The following physical constants were employed:

iodine decay constant λ_I	$2.94 \times 10^{-5} \text{ sec.}^{-1}$
xenon decay constant λ_X	$2.10 \times 10^{-5} \text{ sec.}^{-1}$
xenon microscopic thermal absorption cross-section σ_X	$2.60 \times 10^{-18} \text{ cm}^2.$
xenon fractional fission yield γ_X	0.003
iodine fractional fission yield γ_I	0.0586

The iodine cross-section is so small that iodine burn-out is ignored in comparison with iodine decay.

XEN01747 also includes the reactor height or radius (cm.), the fraction of this linear dimension over which the fundamental flux is flattened (dimensionless), the migration area M^2 (cm^2), the ratio of the fission cross-section to the fission + capture cross-section (dimensionless; FORTRAN mnemonic SIGRAT), and the power (temperature) coefficient (in units of k/unit flux). For the Mark XIIIA-50A,B,

reactor height H	$= 381 \text{ cm.}$
reactor radius R	$= 256 \text{ cm.}$
M^2	$= 260 \text{ cm}^2.$ at start of cycle
M^2	$= 317 \text{ cm}^2.$ at end of cycle.

Fractional flattening of the fundamental flux was allowed to range from zero (cosine or J_0 fundamental) to unit (100% flat); a value of 0.50 probably represents actual conditions fairly well.

The reactivity held in xenon is

$$\rho_x = \frac{k'_{\text{eff}} - k_{\text{eff}}}{k'_{\text{eff}}}$$

$$= \frac{f' - f}{f'} \quad (\text{assuming no Xe effect on } \eta, \epsilon, \rho)$$

~~SECRET~~

UNCLASSIFIED

~~SECRET~~
UNCLASSIFIED

where k'_{eff} and k_{eff} are the effective multiplication factors with and without xenon, respectively, and f' and f are the corresponding values of the thermal utilization. For a homogeneous or a uniformly-loaded reactor,

$$f = \frac{\Sigma_{aF}}{\Sigma_{aF} + \Sigma_{aM}} \quad (\text{no Xe})$$

and

$$f' = \frac{\Sigma_{aF}}{\Sigma_{aF} + \Sigma_{aM} + \Sigma_x} \quad (\text{with Xe})$$

where

- Σ_{aF} = macroscopic absorption cross-section of fuel
- Σ_{aM} = macroscopic absorption cross-section of moderator
- Σ_x = macroscopic absorption cross-section of xenon.

The reactivity is then given by

$$\rho_x = \frac{-\Sigma_x / \Sigma_{aF}}{1 + \Sigma_{aM} / \Sigma_{aF}}$$

$$\cong -\frac{\Sigma_x}{\Sigma_{aF}} = -P \quad \text{for } \Sigma_{aM} \ll \Sigma_{aF}$$

where P is the poisoning due to xenon. The equilibrium value of the xenon poisoning is

$$P^0 = \frac{N_x^0 \sigma_x}{\Sigma_{aF}} = \frac{\sigma_x (\gamma_I + \gamma_x) \Sigma_f \phi^0}{(\lambda_x + \sigma_x \phi^0) \Sigma_{aF}}$$

$$\cong (\gamma_I + \gamma_x) \frac{\Sigma_f}{\Sigma_{aF}} \quad \text{for large } \phi^0 \text{ (i.e., saturated Xe),}$$

where Σ_f is the macroscopic fission cross section.

~~SECRET~~
UNCLASSIFIED

Hence the reactivity held in saturated Xe is

$$\alpha_x = -\rho_{x,\text{sat}} = \frac{(\gamma_I + \gamma_x) \Sigma_f / \Sigma_{aF}}{1 + \Sigma_{aM} / \Sigma_{aF}} \approx (\gamma_I + \gamma_x) \frac{\Sigma_f}{\Sigma_{aF}}$$

Since XEN01747 computes α_x by

$$\alpha_x = (\gamma_I + \gamma_x)(\text{SIGRAT})$$

the input value of SIGRAT is given by

$$\text{SIGRAT} = \frac{\Sigma_f / \Sigma_{aF}}{1 + \Sigma_{aM} / \Sigma_{aF}} \approx \frac{\Sigma_f}{\Sigma_{aF}}$$

for a homogeneous or uniformly-loaded reactor.

If, however, the reactor is heterogeneous (mixed lattice), with separate fuel, moderator, and target regions, the thermal utilization values are

$$f = \frac{\int \Sigma_{aF} \phi dV}{\int (\Sigma_{aF} + \Sigma_{aM} + \Sigma_{aT}) \phi dV} = \frac{\Sigma_{aF}}{\Sigma_{aF} + \frac{V_M \bar{\phi}_M}{V_F \bar{\phi}_F} \Sigma_{aM} + \frac{V_T \bar{\phi}_T}{V_F \bar{\phi}_F} \Sigma_{aT}}$$

and

$$f' = \frac{\int \Sigma_{aF} \phi dV}{\int (\Sigma_{aF} + \Sigma_{aM} + \Sigma_{aT} + \Sigma_x) \phi dV} = \frac{\Sigma_{aF}}{\Sigma_{aF} + \frac{V_M \bar{\phi}_M}{V_F \bar{\phi}_F} \Sigma_{aM} + \frac{V_T \bar{\phi}_T}{V_F \bar{\phi}_F} \Sigma_{aT} + \Sigma_x}$$

where the average thermal fluxes have been defined as

$$\bar{\phi}_F = \frac{1}{V_F} \int_{V_F} \phi dV, \quad \bar{\phi}_M = \frac{1}{V_M} \int_{V_M} \phi dV, \quad \bar{\phi}_T = \frac{1}{V_T} \int_{V_T} \phi dV.$$

In the above equations the relative fuel and target flux values have been assumed to be independent of the xenon poison.

The xenon reactivity is then given by

$$\rho_x = \frac{-\Sigma_x / \Sigma_{aF}}{1 + C_1 \frac{\Sigma_{aM}}{\Sigma_{aF}} + C_2 \frac{\Sigma_{aT}}{\Sigma_{aF}}}$$

where

$$C_1 = V_M \bar{\phi}_M / V_F \bar{\phi}_F$$

$$C_2 = V_T \bar{\phi}_T / V_F \bar{\phi}_F$$

so that the input value of SIGRAT is

$$\text{SIGRAT} = \frac{\Sigma_f / \Sigma_{aF}}{1 + C_1 \frac{\Sigma_{aM}}{\Sigma_{aF}} + C_2 \frac{\Sigma_{aT}}{\Sigma_{aF}}} = \frac{\Sigma_f / \Sigma_{aF}}{1 + \epsilon}$$

rather than Σ_f / Σ_{aF} as for the homogeneous or uniformly-loaded reactor.

Actually the average thermal flux ratios are not constant. Since xenon is produced only in the fuel, $\bar{\phi}_F$ will be depressed and the ratios $\bar{\phi}_M / \bar{\phi}_F$ and $\bar{\phi}_T / \bar{\phi}_F$ will be raised. This enhancement effect may be formally represented by writing

$$\bar{\phi}_M / \bar{\phi}_F \text{ with no Xe} \longrightarrow (1+R) \bar{\phi}_M / \bar{\phi}_F \text{ with saturated Xe,}$$

$$\bar{\phi}_T / \bar{\phi}_F \text{ with no Xe} \longrightarrow (1+R) \bar{\phi}_T / \bar{\phi}_F \text{ with saturated Xe.}$$

The thermal utilization in the absence of xenon is still given by

$$f = \frac{\Sigma_{aF}}{\Sigma_{aF} + C_1 \Sigma_{aM} + C_2 \Sigma_{aT}}$$

but now, with saturated xenon,

$$f' = \frac{\Sigma_{aF}}{\Sigma_{aF} + (1+R)C_1 \Sigma_{aM} + (1+R)C_2 \Sigma_{aT} + \Sigma_{x,sat}} = f'_{sat}$$

$$\begin{aligned} \text{Then } \rho_{x, \text{sat}} &= \frac{f'_{\text{sat}} - f}{f'_{\text{sat}}} \\ &= \frac{-RC_1 \Sigma_{aM} - RC_2 \Sigma_{aT} - \Sigma_{x, \text{sat}}}{\Sigma_{aF} + C_1 \Sigma_{aM} + C_2 \Sigma_{aT}} \end{aligned}$$

which of course reduces to the non-enhanced heterogeneous expression

$$\rho_x = \frac{-\Sigma_x / \Sigma_{aF}}{1 + C_1 \frac{\Sigma_{aM}}{\Sigma_{aF}} + C_2 \frac{\Sigma_{aT}}{\Sigma_{aF}}}$$

as R goes to zero. Including this enhancement effect for the heterogeneous reactor leads to an input SIGRAT given by

$$\text{SIGRAT} = \frac{\Sigma_f / \Sigma_{aF}}{1 + \epsilon} + \left(\frac{R}{\gamma_I + \gamma_x} \right) \left(\frac{\epsilon}{1 + \epsilon} \right)$$

which reduces to $(\Sigma_f / \Sigma_{aF}) / (1 + \epsilon)$ for small R, as it should. This enhancement effect⁽³⁾ can be closely approximated by

$$\text{SIGRAT} = 1.5 \left(\frac{\Sigma_f / \Sigma_{aF}}{1 + \epsilon} \right).$$

Evaluation with the HAMMER and HERESY codes gives

$$\text{SIGRAT} = 1.5 \left(\frac{0.737}{1 + 0.81} \right) = 0.611$$

for the Mark XIIIA-50A lattice.

Power coefficients (in units of k/unit flux) were calculated for the axial and the radial modes of oscillation as follows:

- (a) the Doppler coefficient of U^{235} was taken as zero.
- (b) from the Mark XIIA-50A Technical Manual (3), the moderator temperature coefficient was taken to be -5×10^{-5} k/°C over the whole cycle; assuming that the moderator temperature rises from 20°C at zero power to 90°C at 1900 MW, and that at this power the average flux over the whole cycle is 2.7×10^{14} n/cm².sec.,* the moderator power coefficient becomes

$$\left(-5 \times 10^{-5} \frac{\text{k}}{^\circ\text{C}}\right) \left(\frac{90 - 20}{1900} \frac{^\circ\text{C}}{\text{MW}}\right) \left(\frac{1900 \text{ MW}}{2.7 \times 10^{14} \text{ n/cm}^2 \cdot \text{sec.}}\right)$$

$$= -1.30 \times 10^{-17} \frac{\text{k}}{\text{n/cm}^2 \cdot \text{sec.}}$$

- (c) from the Technical Manual, the coolant temperature coefficient was taken to be -11×10^{-5} k/°C over the whole cycle; assuming that the coolant temperature rises from 20°C at zero power to 60°C at 1900 MW, the coolant power coefficient becomes

$$\left(-11 \times 10^{-5} \frac{\text{k}}{^\circ\text{C}}\right) \left(\frac{60 - 20}{1900} \frac{^\circ\text{C}}{\text{MW}}\right) \left(\frac{1900 \text{ MW}}{2.7 \times 10^{14} \text{ n/cm}^2 \cdot \text{sec.}}\right)$$

$$= -1.63 \times 10^{-17} \frac{\text{k}}{\text{n/cm}^2 \cdot \text{sec.}}$$

- (d) Then for axial oscillations, the power coefficient α_T was taken as the coolant power coefficient only, i.e., axial $\alpha_T = -1.63 \times 10^{-17}$ k/unit ϕ . Clearly the coolant temperature profile will reflect any changes in power distribution along the length of the fuel assemblies. But the moderator temperature coefficient must not be included, because for operation at constant total power, the coolant inlet and outlet temperatures are unchanged, so that the bulk moderator temperature will not be affected by axial power redistributions.

*initial average flux = 2.05×10^{14} n/cm².sec.,
 final average flux = 3.35×10^{14} n/cm².sec.

- (e) for radial oscillations. the power coefficient α_T must include not only the coolant temperature coefficient but also some fraction of the moderator temperature coefficient. Radial remixing of the bulk moderator is not complete, as is demonstrated by the fact that radial oscillations were indeed detected (cf. p. 16) by fluctuating differences in observed moderator temperatures between opposite sectors of the reactor. To allow for partial remixing, only an arbitrary $2/3$ of the moderator coefficient was added to the coolant coefficient, so that the radial $\alpha_T =$
- $$-1.63 \times 10^{-17} + \frac{2}{3} (-1.30 \times 10^{-17}) = -2.50 \times 10^{-17}$$
- k/unit ϕ .

II. Calculation of Flux Thresholds

Axial Oscillations

Typical values of the threshold flux and corresponding oscillation periods at threshold are listed in Table I for axial oscillations. Complete axial threshold results are shown in Figures 1 and 2.

At the start of the cycle, $M^2 = 260 \text{ cm}^2$. and the axial flux fundamental is about 80% flattened, but the flattening can vary with the way the control system is used. With a negative temperature coefficient, two flux thresholds exist (line 3, Table I): a lower threshold at $5.36 \times 10^{13} \text{ n/cm}^2 \cdot \text{sec.}$, and an upper threshold, at $7.84 \times 10^{14} \text{ n/cm}^2 \cdot \text{sec.}$, which arises because xenon saturates at high flux while the effect of the temperature coefficient does not. Below the lower threshold and above the upper threshold, any oscillation caused by some asymmetric perturbation will decay, but between these thresholds, any oscillation will grow (just at either threshold, any oscillation will maintain itself with constant amplitude).

Table I

Flux Thresholds for Axial Oscillations

$$H = 381 \text{ cm.}, \sigma_x = 2.60 \times 10^{-18} \text{ cm}^2., \text{SIGRAT} = 0.611$$

Cycle	M ² cm ²)	Fraction Flat	α_T (k/ ϕ)	Single or Lower ϕ th (n/cm ² sec.)	Period (hours)	If $\alpha_T < 0$, Upper ϕ th (n/cm ² sec.)	Period (hours)	Sustained Oscillations Possible?
start	260	0	-1.63×10^{-17}	none	-	none	-	no
start	260	0.50	-1.63×10^{-17}	none	-	none	-	no
start	260	0.80	-1.63×10^{-17}	5.36×10^{13}	23.3	7.84×10^{14}	7.1	yes
end	317	0	-1.63×10^{-17}	none	-	none	-	no
end	317	0.50	-1.63×10^{-17}	None	-	none	-	no

Since the initial operating average flux, 2.05×10^{14} n/cm².sec., lies between these threshold fluxes, this lattice will indeed be susceptible to axial xenon oscillations at the start of the cycle.

If the temperature coefficient had been zero, the reactor would have been somewhat more unstable, as shown by the lower oscillation threshold of 4.88×10^{13} n/cm²sec. when 80% flattened.

At the end of the cycle, M² has increased to 317 cm². and the fundamental flux is almost unflattened. The reactor is no longer susceptible to axial oscillations (line 4).

The data in Table I and Figures 1 and 2 show that

- (a) stability is slightly improved by a negative temperature coefficient;
- (b) stability is quite adversely affected by increased flux flattening;
- (c) stability is markedly improved by a larger value of the migration area.

FIG. 1

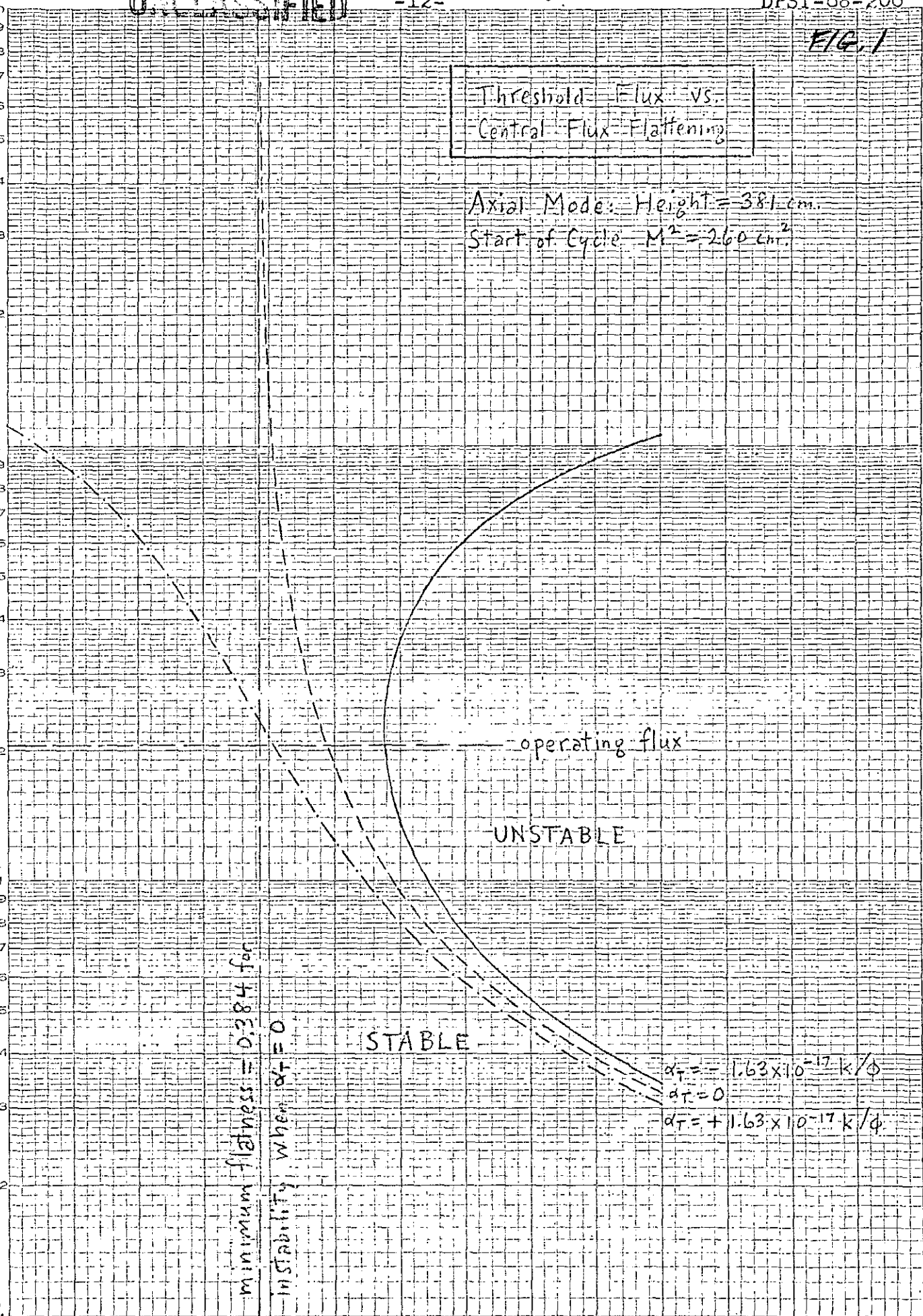
Threshold Flux vs. Central Flux Flattening

Axial Mode: Height = 381 cm.
Start of Cycle $M^2 = 2.60 \text{ cm}^2$

Threshold Flux, $n/\text{cm}^2\text{-sec.}$

10^{13}

10^{16}



minimum flatness = 0.384 for instability when $dT = 0$

operating flux

UNSTABLE

STABLE

$$\frac{dT}{dt} = -1.63 \times 10^{-17} k/\phi$$

$$\frac{dT}{dt} = 0$$

$$\frac{dT}{dt} = +1.63 \times 10^{-17} k/\phi$$

0 0.20 0.40 0.60 0.80 1.00 (flat)

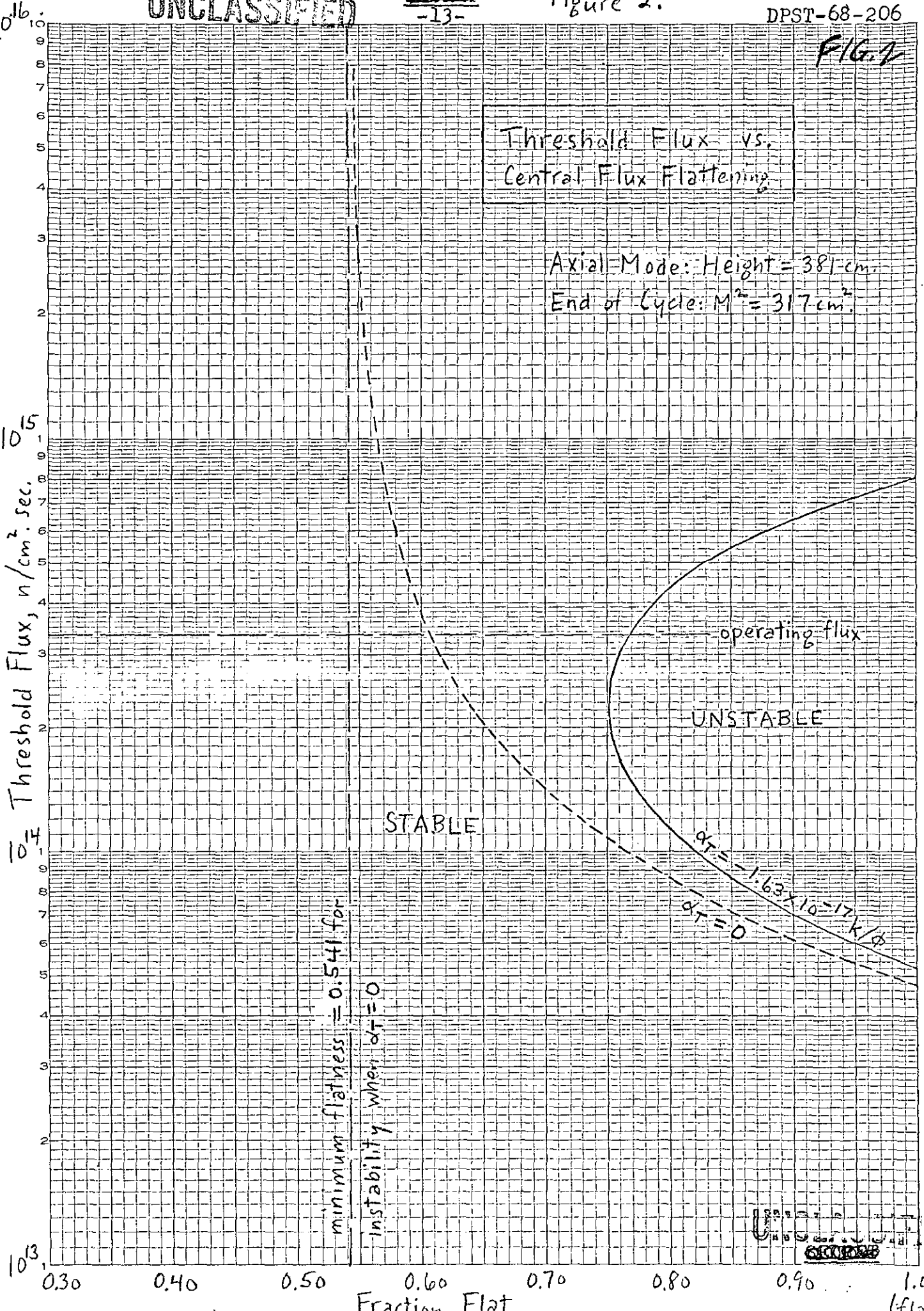
EUBENE DIETZGEN CO. MADE IN U.S.A.

NO. 341-LS10 DIETZGEN GRAPH PAPER SEMI-LOGARITHMIC - 3 CYCLES X 70 DIVISIONS

FIG. 2

Threshold Flux vs. Central Flux Flattening

Axial Mode: Height = 381 cm.
End of Cycle: $M^2 = 317 \text{ cm}^2$



Threshold Flux, $n/cm^2 \cdot sec$

STABLE

UNSTABLE

operating flux

minimum flatness = 0.541 for instability when $\alpha_T = 0$

$\alpha_T = 1.63 \times 10^{-17} k/A$

$\alpha_T = 0$

Fraction Flat

EUGENE DIETZGEN CO.
MADE IN U.S.A.

NO. 341-L310 DIETZGEN GRAPH PAPER
SEMI-LOGARITHMIC-3 CYCLES X 70 DIVISIONS

UNCLASSIFIED

These conclusions are strikingly illustrated in Figures 1 and 2. Points lying in a region to the left of a particular curve represent stable flux-flatness combinations; areas to the right are regions of instability. Figure 1 shows three such curves, at the start of the cycle: one for the expected negative temperature coefficient, one for a hypothetical zero temperature coefficient, and one for a hypothetical positive temperature coefficient of the same magnitude but opposite sign as the expected value. This latter case shows the smallest stable region and in fact predicts a threshold flux for all degrees of flattening right down to zero (where the fundamental flux is cosine-shaped and most resistant to xenon oscillations). The $\alpha_T = 0$ curve bounds a larger region of stability; in this case, no sustained xenon oscillations are possible at any flux level, unless the fundamental flux is more than 38.4% flattened. The negative α_T curve encloses the smallest region of instability: for greater than 57.5% flattening, two thresholds exist, so that if the operating flux lies between them, oscillations will grow; if the operating flux lies below the lower threshold or above the upper threshold, oscillations will decay; just on the line (for this or any other value of α_T), sustained oscillations of constant amplitude can occur.

Figure 2 shows similar curves at the end of the cycle, but only for α_T equal to zero and to its expected negative value. The increased migration area has shifted both curves to the right, so that for a given value of α_T , the region of stability has increased. Now, for $\alpha_T = 0$, sustained oscillations are impossible at any flux level unless the fundamental flux is more than 54.1% flattened; and for $\alpha_T = -1.63 \times 10^{-17} \text{ k}/\phi$, no thresholds exist unless the fundamental is more than 75.1% flat.

Radial Oscillations

Table II lists typical values of the threshold flux and corresponding periods at threshold for radial oscillations. Complete radial threshold results are shown in Figures 3 and 4.

At the start of the cycle, $M^2 = 260 \text{ cm}^2$ and the radial flux fundamental is about 60% flattened. With a negative temperature coefficient, two flux thresholds exist (line 3, Table II): a lower threshold at $5.03 \times 10^{13} \text{ n/cm}^2 \text{ sec.}$, and an upper threshold at $5.26 \times 10^{14} \text{ n/cm}^2 \text{ sec.}$ Since the initial operating average flux, $2.05 \times 10^{14} \text{ n/cm}^2 \text{ sec.}$, lies between these threshold fluxes, the lattice is susceptible to radial xenon oscillations at the start of the cycle. Moreover, it is slightly more susceptible to radial than to axial oscillations, because the lower radial threshold, $5.03 \times 10^{13} \text{ n/cm}^2 \text{ sec.}$, is a little smaller than the lower axial threshold, $5.36 \times 10^{13} \text{ n/cm}^2 \text{ sec.}$

If the temperature coefficient had been zero, the reactor would have been somewhat more unstable, as shown by a lower oscillation threshold of $4.41 \times 10^{13} \text{ n/cm}^2 \text{ sec.}$ when 60% flattened.

Table II

Flux Thresholds for Radial Oscillations

$$R = 256 \text{ cm.}, \sigma_x = 2.60 \times 10^{-18} \text{ cm}^2., \text{SIGRAT} = 0.611$$

Cycle	M ² (cm ²)	Fraction Flat	α_T (k/ ϕ)	Single or Lower ϕ_{th} (n/cm ² sec.)	Period (hours)	If $\alpha_T < 0$, Upper ϕ_{th} (n/cm ² sec.)	Period (hours)	Sustained Oscillation Possible?
start	260	0	-2.50x10 ⁻¹⁷	none	-	none	-	no
start	260	0.50	-2.50x10 ⁻¹⁷	7.33x10 ¹³	20.8	3.95x10 ¹⁴	9.8	yes
start	260	0.60	-2.50x10 ⁻¹⁷	5.03x10 ¹³	23.8	5.26x10 ¹⁴	8.6	yes
end	317	0	-2.50x10 ⁻¹⁷	none	-	none	-	no
end	317	0.50	-2.50x10 ⁻¹⁷	none	-	none	-	no
end	317	0.60	-2.50x10 ⁻¹⁷	1.07x10 ¹⁴	17.8	2.87x10 ¹⁴	11.5	no!

At the end of the cycle, M² has increased to 317 cm², but the fundamental flux still remains about 60% flattened. The lower threshold flux has been raised from 5.03 x 10¹³ n/cm² sec. to 1.07 x 10¹⁴ n/cm² sec. and the upper threshold flux lowered from 5.26 x 10¹⁴ n/cm² sec to 2.87 x 10¹⁴ n/cm² sec. (line 6). Simultaneously the operating average flux has risen from 2.05 x 10¹⁴ n/cm² sec. to 3.35 x 10¹⁴ n/cm² sec., so that it now lies above the upper threshold; the reactor is now stable at full power. However, oscillations still could occur during power ascension from a scram recovery.

If the fundamental flux were flattened to the same extent both axially and radially, say 50%, the reactor would be distinctly more susceptible to radial than to axial observations. With zero temperature coefficients, the radial threshold 5.89 x 10¹³ n/cm² sec. is lower than the axial threshold 1.86 x 10¹⁴ n/cm² sec. at the start of the cycle; at the end of the cycle, sustained axial oscillations are no longer possible, although a radial threshold, 1.18 x 10¹⁴ n/cm² sec., still exists. With the respective negative temperature coefficients, sustained axial oscillations are impossible at both the start and the end of the cycle, although radial oscillations are possible (threshold flux = 7.33 x 10¹³ n/cm² sec.) at the start (but not the end) of the cycle.

UNCLASSIFIED

~~SECRET~~

-16-

P. L. ROGGENKAMP

DPST-68-206

Figures 3 and 4 (analogous to Figures 1 and 2 for the axial case) map the stable and unstable regions for the radial mode, at the start and at the end of the cycle, respectively. Here again, the larger migration area at the end of the cycle has shifted the curves to the right, decreasing the region of instability. Thus for the expected negative temperature coefficient, the minimum flattening for radial oscillation thresholds has been raised from 40.3% at the start of the cycle to 57.0% at the end of the cycle. If $\alpha_T = 0$, the reactor exhibits an oscillation threshold for all degrees of flattening at the start of the cycle, but by the end of the cycle, the flux must be at least 30.5% flattened for oscillation thresholds to exist.

Note that this does not mean that, if $\alpha_T = 0$, the reactor is subject to radial oscillations for all degrees of flatness at the start of the cycle, or for all degrees of flatness $>30.5\%$ at the end of the cycle. Thresholds do exist under these conditions, but it is not until the flux has been flattened to at least 23.7% (start of cycle) or 38.0% (end of cycle) that the operating average flux equals or exceeds these thresholds, so that radial oscillations become possible. Thus at the start of the cycle, a threshold does exist at 1.98×10^{15} n/cm² sec., but because it is higher than the initial operating flux, sustained radial oscillations are impossible. When $\alpha_T = -2.50 \times 10^{-17}$ k/ ρ , the minimum flattenings for radial oscillations are 40.8% and 62.9% at initial and final operating fluxes of 2.05×10^{14} n/cm² sec. and 3.35×10^{14} n/cm² sec., respectively. The absolute minimum flattening, below which sustained oscillations are impossible at any flux level, is 40.3% at the start and 57.0% at the end of the cycle; these minima could be encountered at flux levels below the operating levels. Similar considerations apply to the axial cases, Figures 1 and 2.

It was reported that radial oscillations were observed (cf. p. 10) with a period of 20 hours at 40% of full power at the start of the cycle. Table III shows the results of a calculation specifically matching these conditions, viz., specified average flux = $(0.40) \times (2.05 \times 10^{14}) = 8.2 \times 10^{13}$ n/cm² sec. at $M^2 = 260$ cm², $\alpha_T = -2.50 \times 10^{-17}$ k/ ρ , $\sigma_x = 2.60 \times 10^{-18}$ cm², SIGRAT = 0.611, and flux flattening = 0.60.

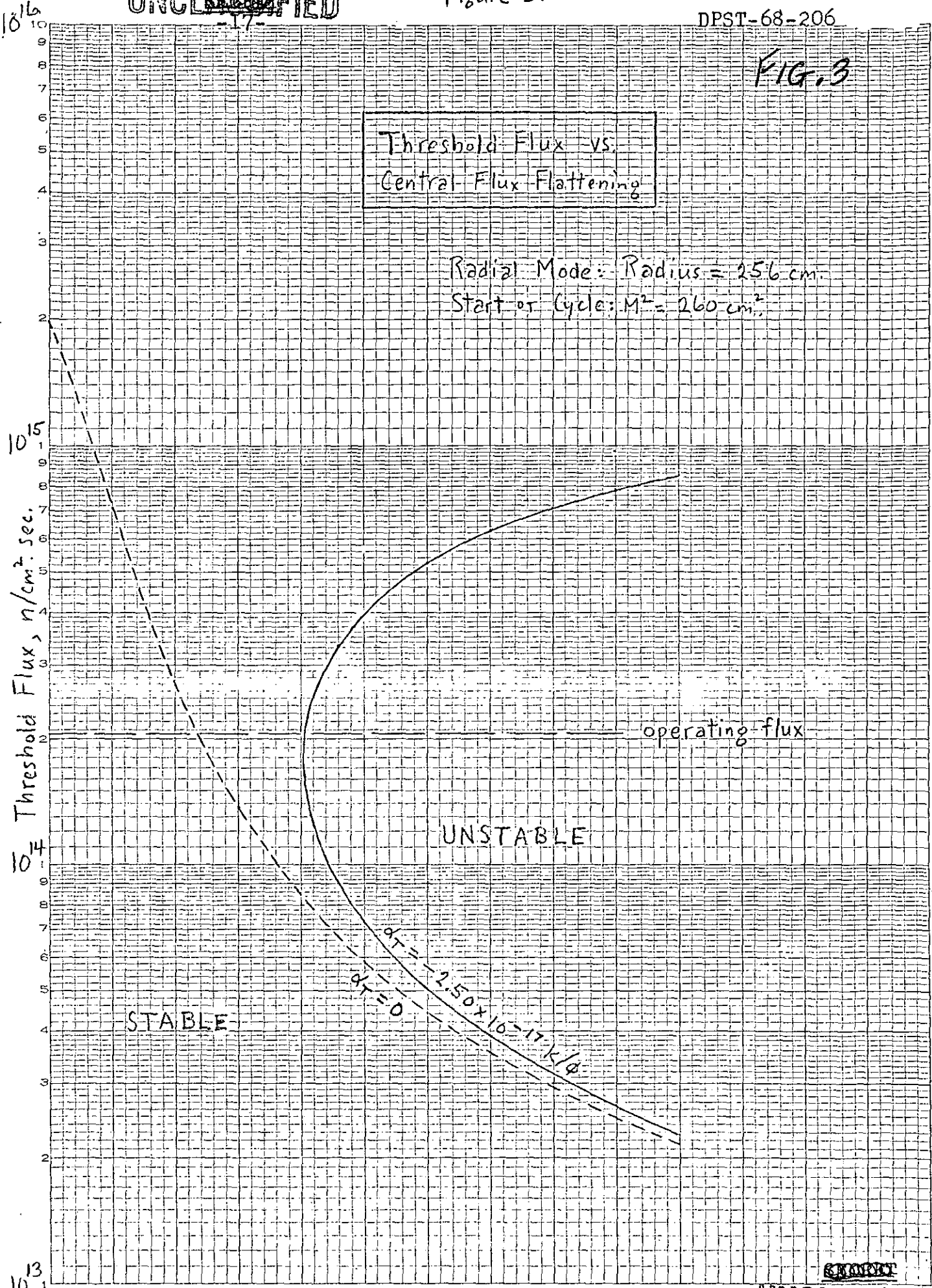
~~SECRET~~

UNCLASSIFIED

FIG. 3

Threshold Flux vs. Central Flux Flattening

Radial Mode: Radius = 256 cm.
Start of Cycle: $M^2 = 260 \text{ cm}^2$



EUGENE DIETZGEN CO.
MADE IN U. S. A.

NO. 341-L310 DIETZGEN GRAPH PAPER
SEMI-LOGARITHMIC-3 CYCLES X 70 DIVISIONS

SECRET

10¹⁶

10¹⁵
Threshold Flux, n/cm².sec.

10¹³

Threshold Flux vs.
Central Flux Flattening

Radial Mode: Radius = 256 cm.
End of Cycle: M² = 317 cm²

operating flux

UNSTABLE

STABLE

$\frac{d\tau}{dt} = -2.50 \times 10^{-17} k/\phi$
 $\frac{d\tau}{dt} = 0$

minimum flatness = 0.305 for
instability when $d\tau = 0$

0.30 0.40 0.50 0.60 0.70 0.80 0.90 1.00
F₀ F₁

EUBENE DIETZGEN CO.
MADE IN U.S.A.

NO. 341-L310 DIETZGEN GRAPH PAPER
SEMI-LOGARITHMIC - 3 CYCLES X 70 DIVISIONS

UNCLASSIFIED

Table III

Calculated vs. Observed Radial Oscillation Period

	Calculated	Observed
Average flux, n/cm ² sec.	8.2 x 10 ¹³ *	8.2 x 10 ¹³ *
Oscillation period, hours	20.2	20
Lower threshold, n/cm ² sec.	5.03 x 10 ¹³	-
Corresponding period, hours	23.8	-
Upper threshold, n/cm ² sec.	5.26 x 10 ¹⁴	-
Corresponding period, hours	8.6	-

*specified equal.

Clearly xenon oscillations could have been observed, since the actual average flux lies between the lower and the upper flux thresholds. The computed oscillation period at this average flux agrees satisfactorily with the observed period. If α_T had been zero, the average flux would have exceeded even more the single threshold flux = 4.41×10^{13} n/cm² sec. (corresponding period = 24.8 hours), and the computed oscillation period at this average flux would have been 21.3 hours (vs. observed 20), rather than 20.2 hours (vs. observed 20) for $\alpha_T = -2.50 \times 10^{-17}$ k/ ϕ .

The observed radial oscillation is shown in Figure 5 where the moderator temperature difference between opposite sectors of the reactor is plotted against time. The value of the first perturbation flux peak can be estimated from the initial ΔT spike of 2°C relative to the average moderator temperature of 45°C:

$$\frac{\phi'}{8.2 \times 10^{13}} = \frac{2^\circ\text{C}}{45^\circ\text{C}}$$

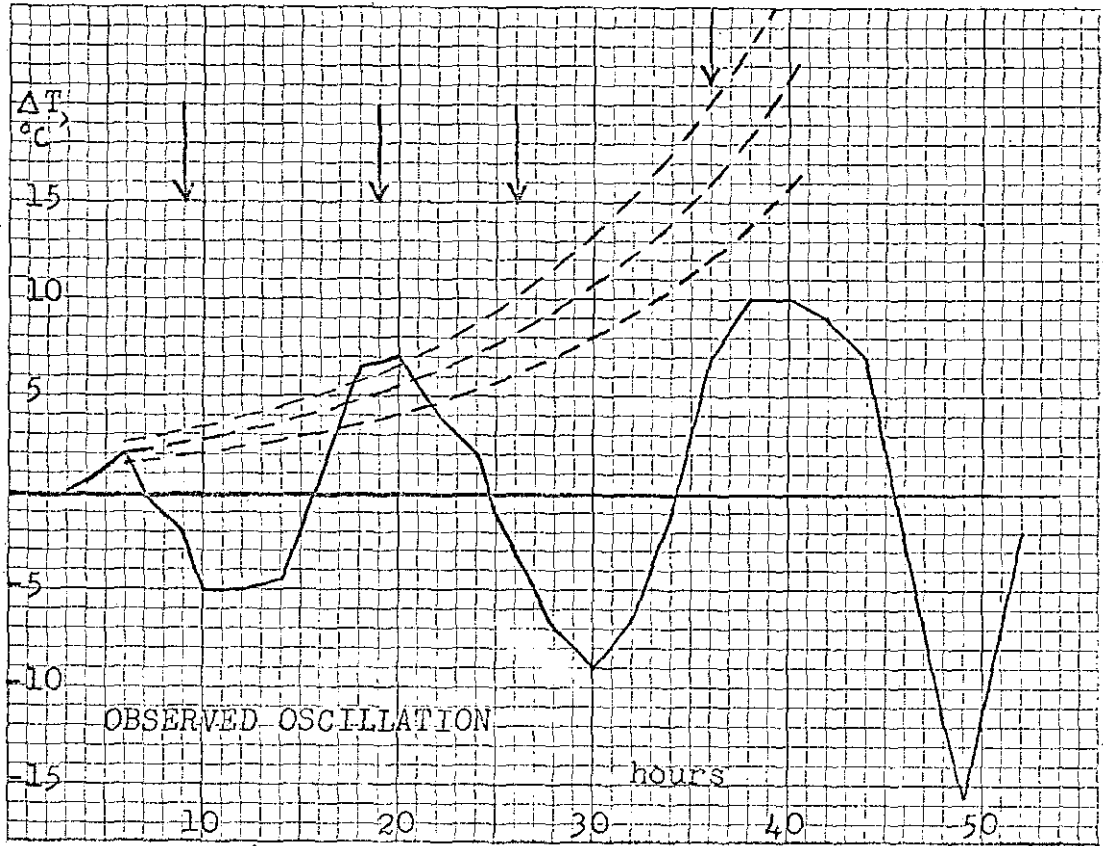
so that the first ϕ' maximum $\cong 4 \times 10^{12}$ n/cm² sec. The time behavior of the perturbation flux is given (1) by

$$\phi' = \phi'' e^{wt}$$

where ϕ'' can now be identified with the first peak, $\phi'' = \phi' = 4 \times 10^{12}$.

UNCLASSIFIED

Figure 5.



UNCLASSIFIED

UNCLASSIFIED

P. L. ROGGENKAMP

~~SECRET~~

-21-

DPST-68-206

The envelope of subsequent peaks in the perturbation flux can then be calculated by

$$\max. \phi' = \phi'' e^{st} = 4 \times 10^{12} \exp(1.93 \times 10^{-5} t)$$

where t is the time in seconds, and $s = \text{Re}(\omega)$ which has been computed by XEN01747 to be $1.93 \times 10^{-5} \text{ sec.}^{-1}$ at the specified flux of $8.2 \times 10^{13} \text{ n/cm}^2 \text{ sec.}^*$ In terms of temperature difference across the reactor,

$$\frac{\Delta T \text{ at } t + \Delta t}{\Delta T \text{ at } t} = \frac{\phi'' e^{s(t + \Delta t)}}{\phi'' e^{st}} = e^{s \Delta t}$$

Taking $\Delta T = 2^\circ\text{C}$ initially, the envelope of subsequent ΔT maxima is given by

$$\max. \Delta T = 2.0 \exp(1.93 \times 10^{-5} t)$$

Because the temperature readings are good to only $\pm 1^\circ\text{C}$, the initial ΔT peak might have been as low as 1.5°C or as high as 2.5°C . Peak ΔT envelopes are plotted as dashed lines in Figure 5 for each of these three initial ΔT peaks. The agreement between the calculated and the observed ΔT maxima is fairly good, especially in view of the fact that attempts were made, at times indicated by the vertical arrows, to damp out these oscillations by control rod movement.

XEN01747 also computes the ratio of any perturbation flux maximum to the subsequent maximum. This amplitude ratio, ϕ_n / ϕ_{n+1} , is 0.25^{**} when the specified average flux is $8.2 \times 10^{13} \text{ n/cm}^2 \text{ sec.}$ This agrees reasonably well with the ratio of the first to the second ΔT peak, namely $2^\circ\text{C}/7^\circ\text{C} = 0.3$, despite corrective control rod action. The third ΔT peak has been so much suppressed that agreement cannot be expected with amplitudes calculated on the basis of a freely-oscillating system.

*the imaginary part of ω is $8.63 \times 10^{-5} \text{ sec.}^{-1}$ corresponding to a period $\tau = 2\pi / \text{Im}(\omega) = 20.2 \text{ hours}$ as in Table III.

**i.e., the oscillation is growing, since each successive perturbation flux amplitude is four times as high as the preceding one.

~~SECRET~~

UNCLASSIFIED

Figure 6 shows a universal plot of threshold flux vs. oscillation period at threshold, for two values of σ_x . It can be shown (4) that at threshold, the oscillation period depends only on the physical constants $\lambda_I, \lambda_X, \gamma_I, \gamma_X$, and σ_x (and of course ϕ_{th}), not on the reactor parameters H or R , M^2 , fraction flat, α_T , and α_x .

The upper curve is based on an average $\sigma_x = 2.60 \times 10^{-18} \text{ cm}^2$ obtained from HAMMER calculations, and used throughout this study (except for Section IV), whereas the lower curve is based on a 2200 m./sec. value* $\sigma_x = 3.08 \times 10^{-18}$ used in previous studies(5).

III. Oscillation Periods for Arbitrary Flux Levels

Oscillations can occur at flux levels above and below, as well as at the threshold (if any) level. Below a lower ($\alpha_T < 0$) or single ($\alpha_T \geq 0$) threshold, an asymmetric power distribution will decay in an oscillatory manner, or if the flux level is sufficiently low, in a steady manner. Above a single threshold, the asymmetry will grow in an oscillatory fashion, or if the flux level is sufficiently high, in a steady manner; ultimately of course this growth will be checked by some non-linear effect (e.g., burnout) which is not taken into account in any perturbation theory treatment. Below an upper threshold ($\alpha_T < 0$), the asymmetry will grow in an oscillatory fashion, but above the upper threshold it will again decay in an oscillatory manner, or steadily if the flux is sufficiently high.

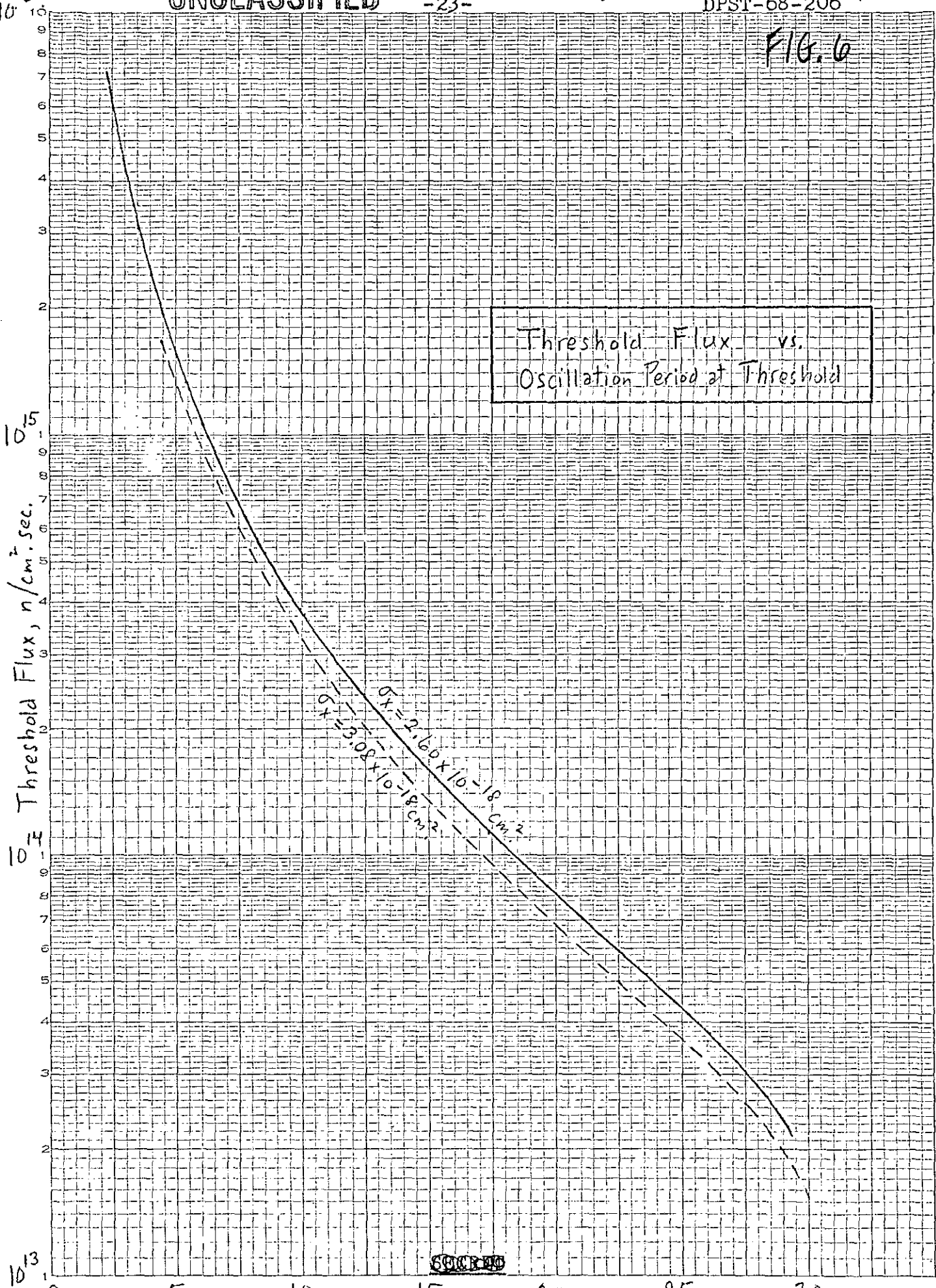
The perturbation flux amplitude ratio ϕ'_n/ϕ'_{n+1} is schematically correlated in Figure 7 with the values of the real and imaginary parts of ω (i.e., $\omega = s + j\sigma$, $j = \sqrt{-1}$) as functions of average flux. For the "no threshold" case, $\phi'_n/\phi'_{n+1} > 1.0$ for all $\sigma > 0$: the maximum amplitude of the $n+1$ th oscillation is always smaller than that of the n th oscillation, and the oscillation decays exponentially with a period $\tau = 2\pi/\sigma$. The real part s has a single negative value within the region of oscillation. Outside of this region, where $\sigma = 0$, s has two negative values, so that the perturbation decays steadily, without oscillation.

If $\alpha_T \geq 0$, only a single threshold is possible. Oscillations can occur wherever $\sigma > 0$. The threshold for divergent oscillations, at which the oscillation is sustained at constant magnitude ($\phi'_n/\phi'_{n+1} = 1.0$), occurs at $s = 0$. Below the threshold, s is single valued and negative, so that the oscillations converge ($\phi'_n/\phi'_{n+1} > 1.0$). Above the threshold, s is single-valued and positive, so that the oscillations diverge ($\phi'_n/\phi'_{n+1} < 1.0$). The perturbation decays or grows steadily when $\sigma = 0$, according as the real roots s are both negative or positive.

*a recent compilation(6) lists several thermal spectrum values for Xe^{135} : $(3.6 \pm 0.4) \times 10^6$, $(3.21 \pm 0.10) \times 10^6$, $(3.2 \pm 1.0) \times 10^6$, 2.4×10^6 , $(2.58 \pm 0.2) \times 10^6$, and $(2.90 \pm 0.13) \times 10^6$ barns; the first is the recommended value.

FIG. 6

Threshold Flux vs. Oscillation Period at Threshold



EUGENE DIETZGEN CO. MADE IN U.S.A.

NO. 941-L310 DIETZGEN GRAPH PAPER SEMI-LOGARITHMIC - 3 CYCLES X 70 DIVISIONS

~~SECRET~~

Figure 7.

Schematic Representation of the Behavior of the Amplitude Ratio and the Roots of the Time-Dependent Perturbation Flux Equation.

$$\phi' = \phi'' e^{i\omega t}$$

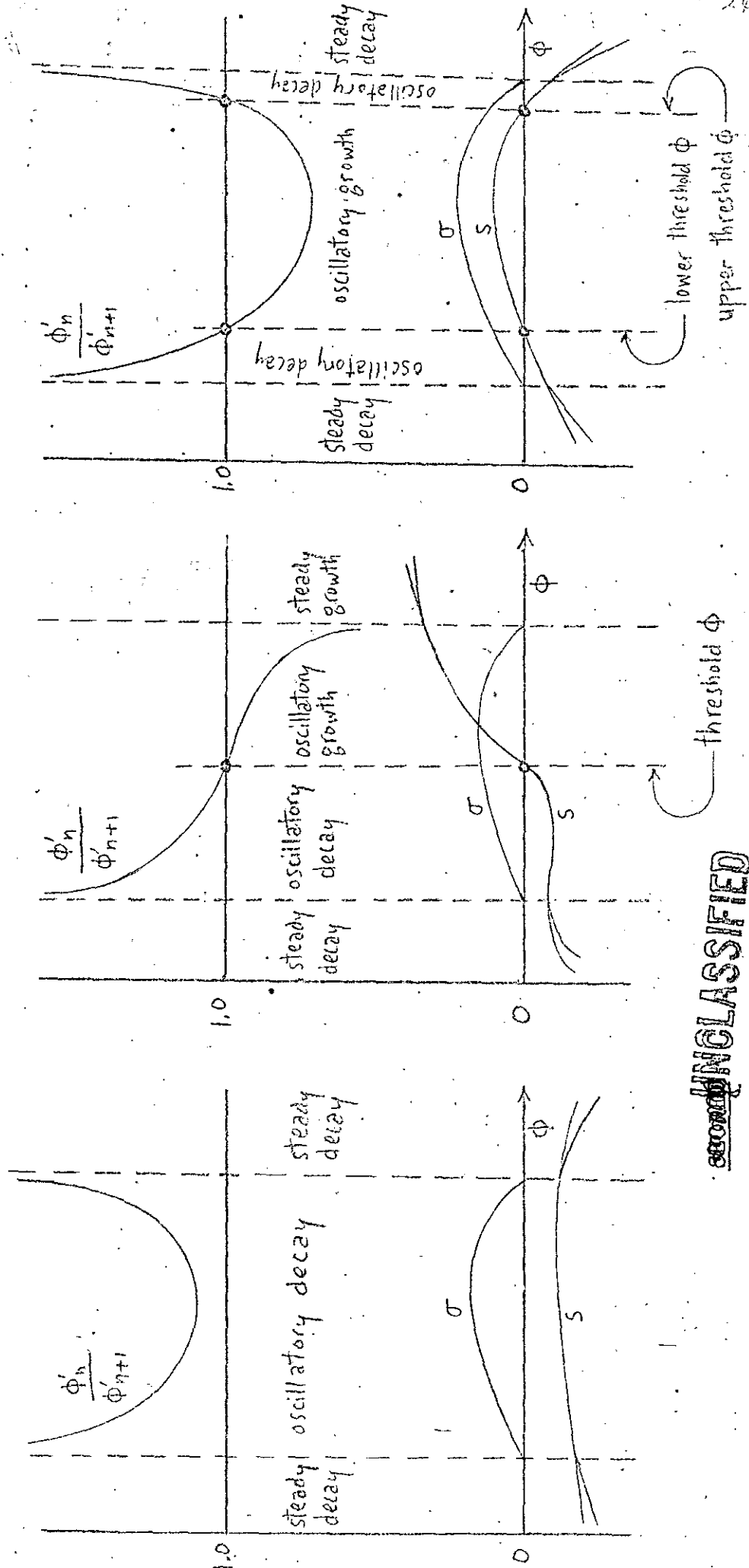
$$\omega = s \pm j\sigma$$

$$\tau = 2\pi/\sigma$$

No. Threshold:
no restriction on $\alpha\tau$

Single Threshold:
 $\alpha\tau \geq 0$

Double Threshold:
 $\alpha\tau < 0$



If $\alpha_T < 0$, a double threshold is generally possible. Below the lower threshold and above the upper threshold, where $\sigma > 0$ and s is single-valued and negative, convergent oscillations occur. Between these two thresholds, where $\sigma > 0$ and s is single-valued and positive, divergent oscillations occur. Outside of the region of oscillation, where $\sigma = 0$, the perturbation decays or grows steadily according as the two real roots s are both negative or positive. Under some conditions*, the two flux thresholds may approach each other until they coincide (the ϕ'_n/ϕ'_{n+1} curve being just tangent to the horizontal 1.0 line); at this precise point, only decaying or just steady oscillations are possible.

Control rod movement is clearly needed to suppress a xenon perturbation whenever the perturbation is growing, either steadily or with oscillation. What is not so apparent is that corrective action may also be required even if the oscillation is decaying. Suppose that the flux level and reactor parameters were such that, if an oscillation were started, then $\phi'_n/\phi'_{n+1} = 2.0$. Suppose further that a local, spatially-unsymmetric drop in reactivity occurred, producing a local 10% reduction in power. This would not do any damage, but one-half a period later, the power would increase locally by about 7%** so that local coolant boiling might result. Only if the reactor is being operated at such a flux level that any induced perturbation would decay steadily (i.e., $\sigma = 0$ and both roots $s < 0$) would control action always be unnecessary.

Oscillation periods are plotted in Figure 8 for axial oscillations at the start of the cycle, assuming a zero temperature coefficient. If the fundamental flux is unflattened, there is no threshold and any asymmetry will decay in an oscillatory manner for flux values in the range $2.8 \times 10^{11} < \phi < 2.8 \times 10^{14}$ n/cm² sec.; above or below these limits (where the period goes to infinity), the decay will be steady. If the fundamental flux is 50% flattened, a threshold exists at 1.86×10^{14} n/cm² sec., and five modes of behavior are possible:

- (a) steady decay for $\phi \leq 1.7 \times 10^{11}$ n/cm² sec.
- (b) oscillatory decay for $1.7 \times 10^{11} < \phi < \phi_{th} = 1.86 \times 10^{14}$ n/cm² sec.
- (c) steady oscillation at $\phi = \phi_{th} = 1.86 \times 10^{14}$ n/cm² sec.
- (d) oscillatory growth for $\phi_{th} = 1.86 \times 10^{14} < \phi < 2.3 \times 10^{15}$ n/cm² sec.
- (e) steady growth for $\phi \geq 2.3 \times 10^{15}$ n/cm² sec.

*e.g., when the flux is 57.5% flattened and $\alpha_T = -1.63 \times 10^{-17}$ k/ ϕ ,

Figure 1; similar conditions are apparent in Figures 2, 3, and 4.

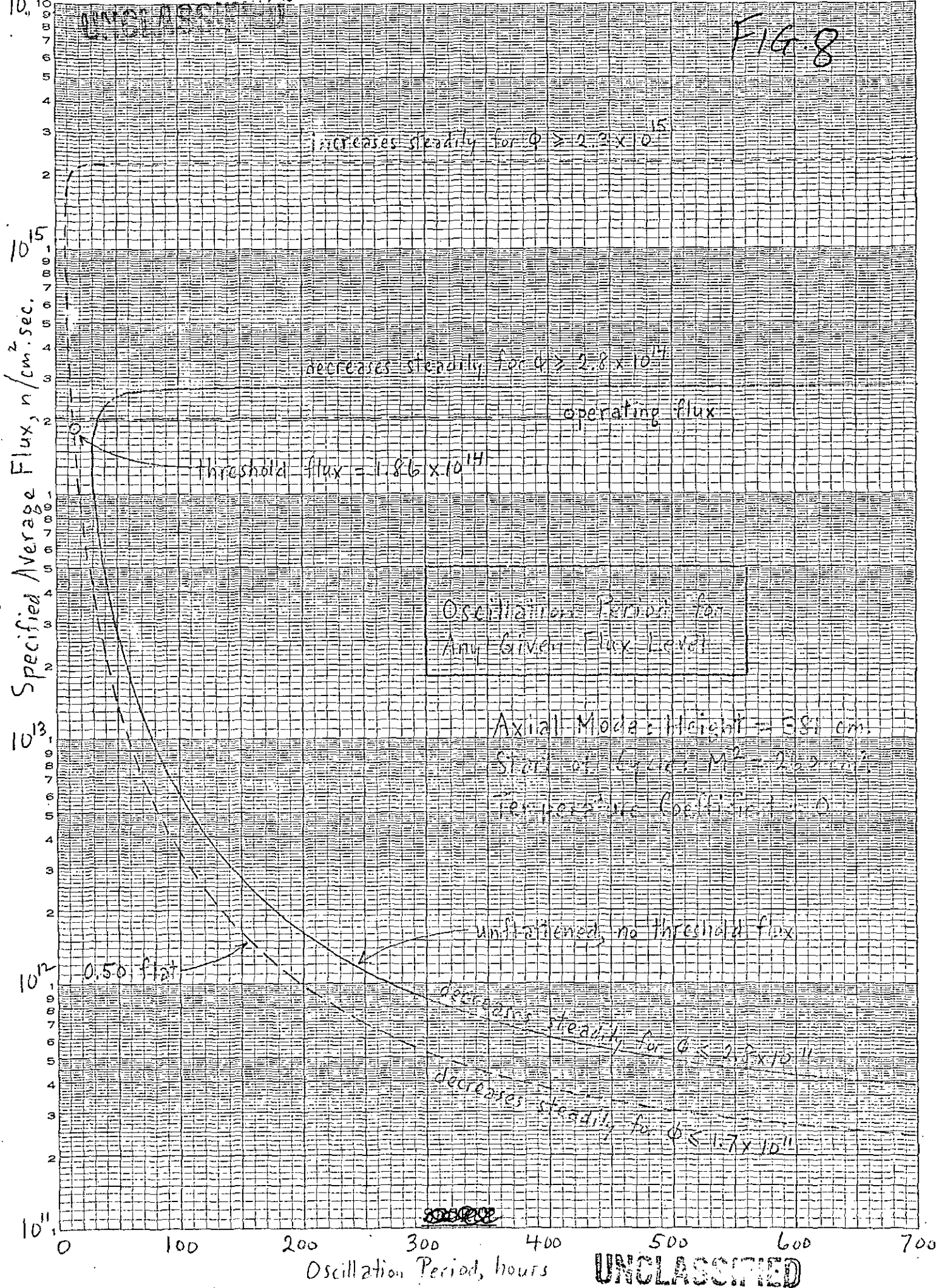
**if $\phi'_1 = -10\%$ when $\phi'_n/\phi'_{n+1} = 2.0$, then $\phi'_2 = -5\%$, and the intermediate maximum ϕ' amplitude =

$$\sqrt{\phi'_1 \phi'_2} = 7\%.$$

FIG. 8

EUGENE DIETZGEN CO.
MADE IN U.S.A.

NO. 340-1.510 DIETZGEN GRAPH PAPER
SEMI-LOGARITHMIC
5 CYCLES X 10 DIVISIONS PER INCH



UNCLASSIFIED

UNCLASSIFIED

~~SECRET~~

-27-

P. L. ROGGENKAMP

DPST-68-206

The mathematical solution of the problem requires that very long periods be possible to allow transition from oscillatory behavior (under-damped) to steady decay or growth (over-damped). At two flux levels the period must go to infinity (critically damped). However, the damping of the perturbation flux (total flux = fundamental flux + perturbation flux) becomes so very large (for $\phi < \phi_{th}$) or so very small (for $\phi > \phi_{th}$) as the actual flux departs from the threshold flux, that long-period oscillations would soon not be recognized as oscillations at all. Thus for the above 50% flattened case, at a flux level of 1×10^{13} n/cm²sec., the ratio of any perturbation flux peak to the next succeeding peak is already 600! The successive amplitudes of such an oscillation fall off so rapidly with each oscillation that the oscillation is quickly submerged in the reactor noise. Conversely, at a flux level of 1×10^{15} n/cm² sec., the perturbation amplitude ratio is only 0.011, which would so closely simulate steady growth that corrective control rod action would be undertaken long before recognition of the oscillatory nature of the perturbation.

The destabilizing effect of flux flattening is illustrated not only by the appearance of a threshold flux at 50% flatness, but also by the wider range of flux levels over which oscillatory behavior can occur, as compared to the zero-flatness curve.

At the end of the cycle, Figure 9, oscillatory decay is observed for all flux levels within $3.3 \times 10^{11} < \phi < 1.225 \times 10^{14}$ n/cm² sec. for zero flatness, or $2.1 \times 10^{11} < \phi < 1.6 \times 10^{16}$ for 50% flatness. No flux threshold appears in either case.

Figures 10 and 11 show oscillation periods vs. flux levels when $\alpha_T = -1.63 \times 10^{-17}$ k/ ϕ , its expected value. The temperature coefficient is sufficiently negative so that no thresholds appear, for either 0 or 50% flattening, at either the start or the end of the cycle. At the start of the cycle, any tilt perturbation on an unflattened fundamental would decay in a theoretically oscillatory but virtually steady manner because of the very long period, about 600 hours; but at the end of the cycle, the zero flatness curve lies wholly beneath the operating average flux, so that any flux tilt perturbation would decay exponentially, without oscillation. On the other hand, if the flux were 50% flat, such flux tilts would decay in an oscillatory manner with periods of 13-14 hours at both the start and the end of the cycle.

Actual amplitude ratios in the vicinity of closest approach to unity are shown in Figures 12 and 13 for axial oscillations at the beginning and end of the cycle, respectively, with α_T assigned its expected negative value. No threshold exists for either zero or 50% flux flattening, although 50% flattening comes much closer

~~SECRET~~

UNCLASSIFIED

decreases steadily for $\phi \geq 1.6 \times 10^{16}$

Figure 9

Oscillation Period for Any Given Flux Level

Axial Moderator Height = 381 cm.
End of Cycle $M^2 = 3.7 \text{ cm}^2$
Temperature Coefficient = 0

operating flux

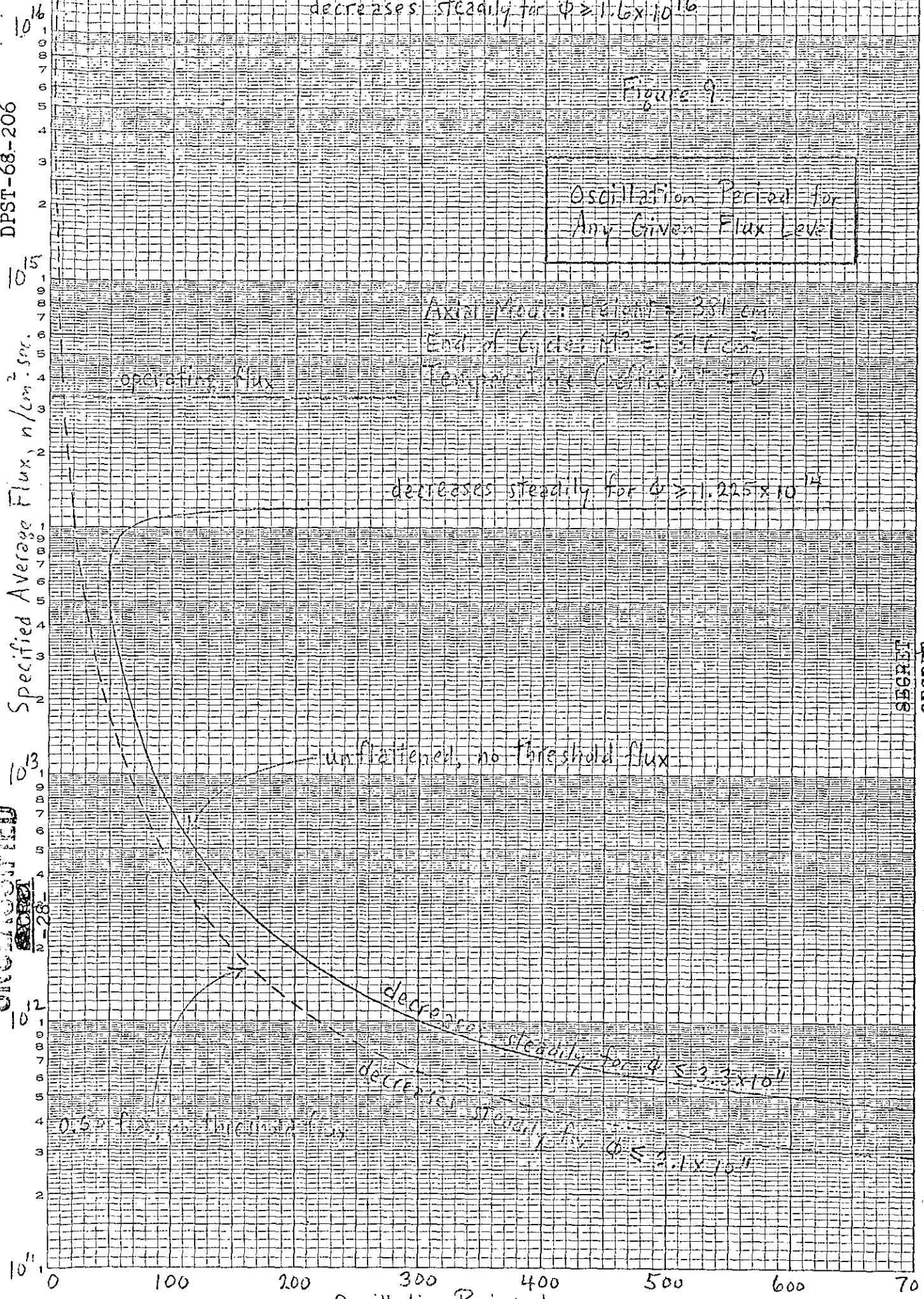
decreases steadily for $\phi \geq 1.225 \times 10^{14}$

unflattened, no threshold flux

decreases steadily for $\phi \leq 3.3 \times 10^{11}$

decreases steadily for $\phi \leq 3.1 \times 10^{11}$

0.5% β , no threshold flux



SECRET

UNCLASSIFIED

Figure 10.

EUGENE DIETZEN CO.
MADE IN U. S. A.

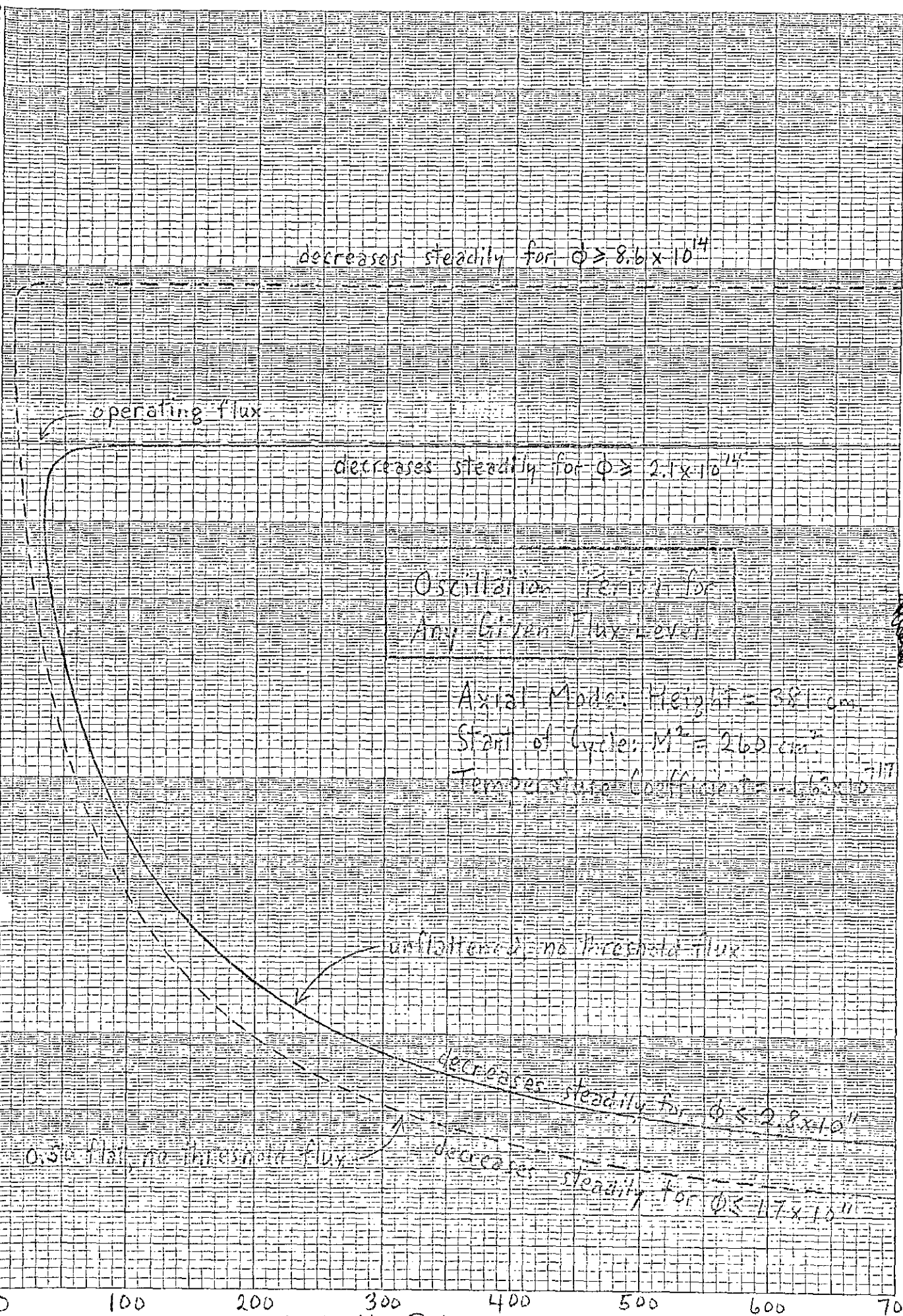
NO. 340-LS10 DIETZEN GRAPH PAPER
5 CYCLES X 10 DIVISIONS PER INCH

DPST-68=206

Specified Average Flux, $n/cm^2 \cdot sec.$

10^{16}
 10^{15}
 10^{14}
 10^{13}
 10^{12}
 10^{11}

10^{11}



decreases steadily for $\phi \geq 8.6 \times 10^{14}$

operating flux

decreases steadily for $\phi \geq 2.1 \times 10^{14}$

Oscillation Period for
Any Given Flux Level

Axial Mode: Height = 381 cm

Start of Cycle: $M^2 = 260 \text{ cm}^2$

Temperature Coefficient = $1.63 \times 10^{-11} \text{ k}/\phi$

unflattened - no threshold flux

0.50 flat - no threshold flux

decreases steadily for $\phi \leq 2.8 \times 10^{11}$

decreases steadily for $\phi \leq 1.7 \times 10^{11}$

Oscillation Period, hours

UNCLASSIFIED

UNCLASSIFIED

SECRET
-30-

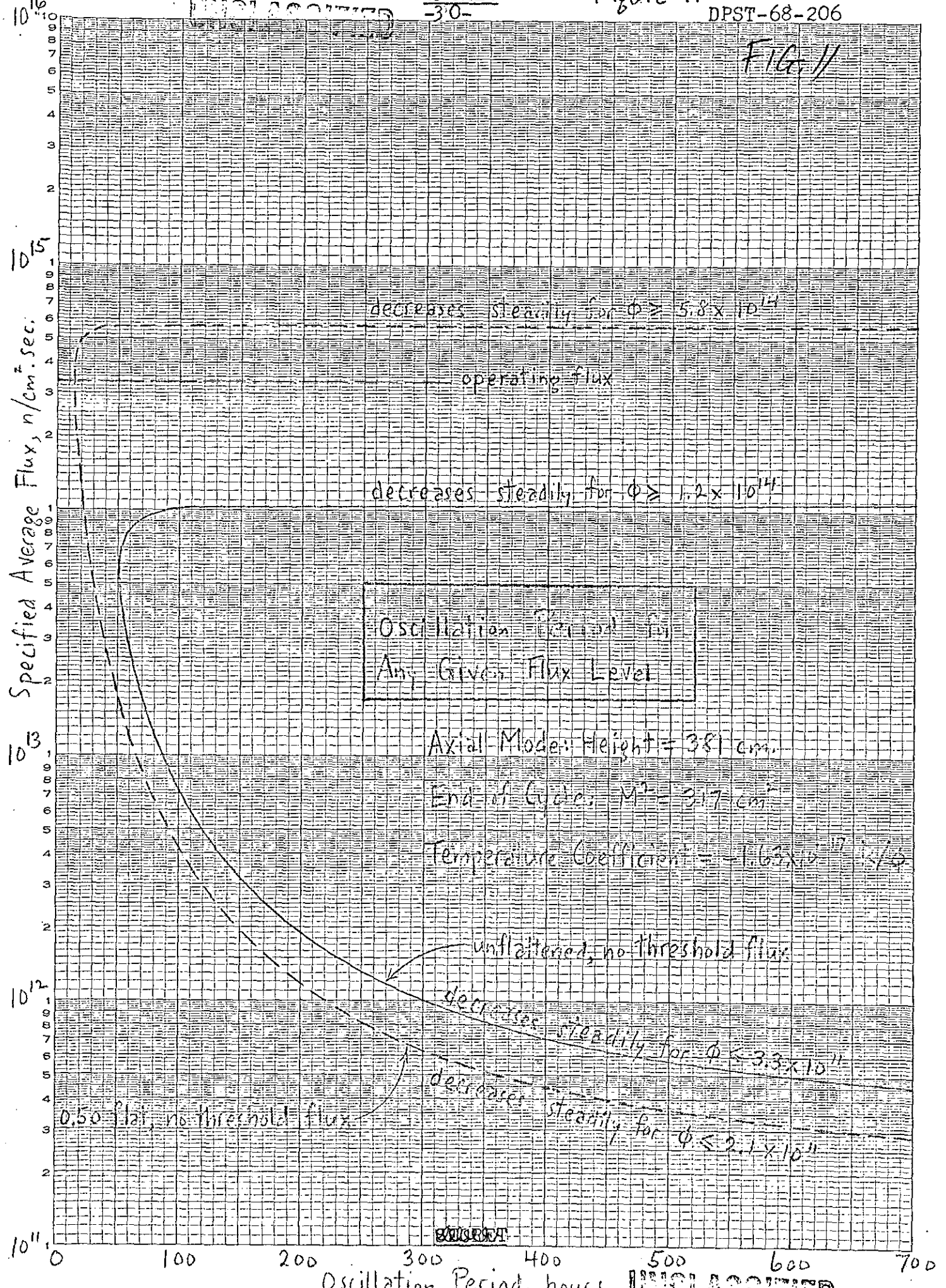
Figure 11.

DPST-68-206

FIG. 11

EUGENE DIETZEN CO.
MADE IN U. S. A.

NO. 340-1510 DIETZEN GRAPH PAPER
SEMI-LOGARITHMIC
5 CYCLES X 10 DIVISIONS PER INCH



UNCLASSIFIED

UNCLASSIFIED

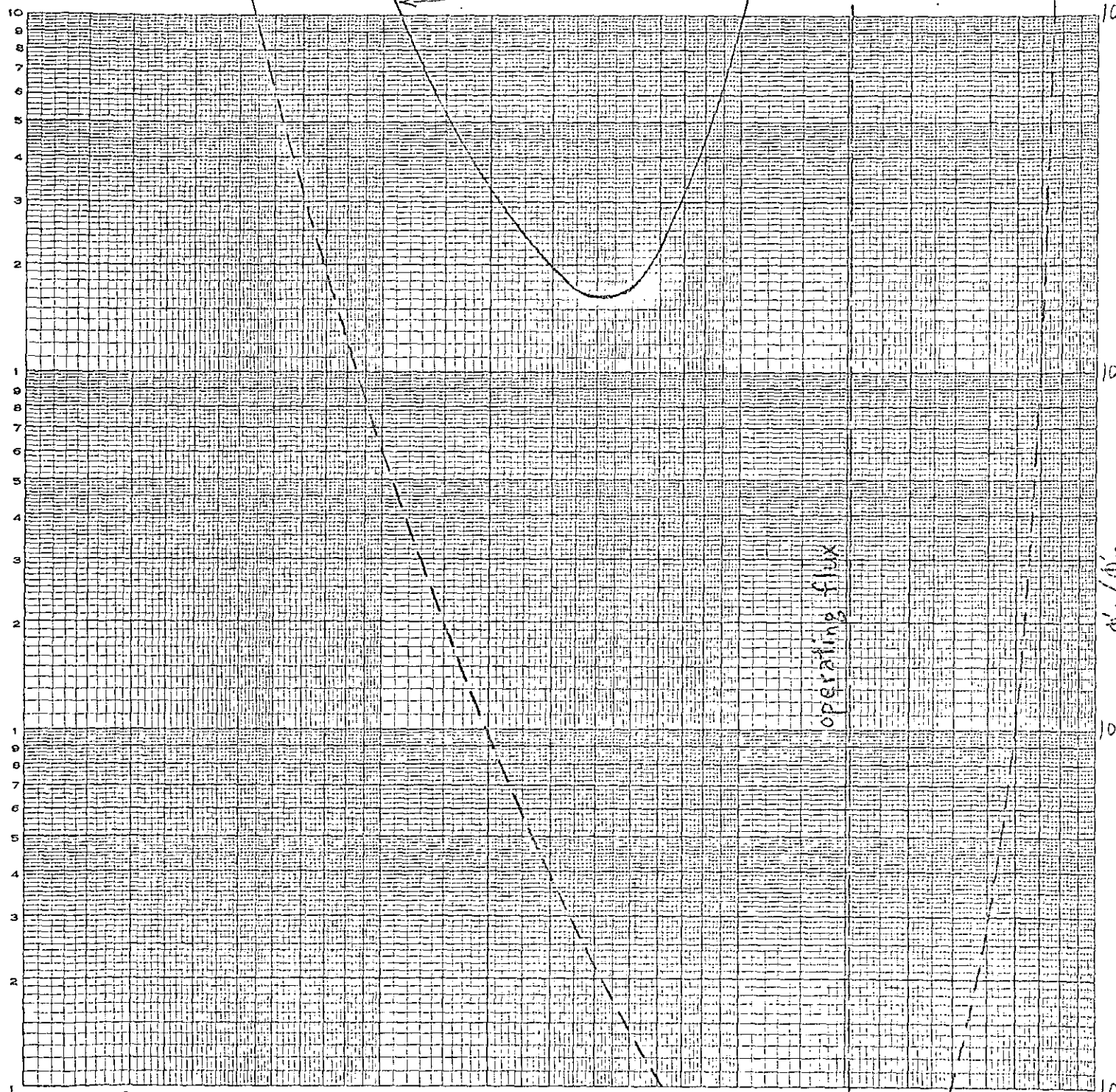
~~SECRET~~
-31-

Perturbation Flux
Amplitude Ratio vs.
Specified Average Flux

Figure 12.
DPST-68-206

0.50 flat

unflattened



Axial Mode: Height = 381 cm.

Start of Cycle: $M^2 = 2.60 \text{ cm}^2$

Temperature Coefficient = $-1.63 \times 10^{-17} \text{ k}/\phi$

No threshold flux in either case.

UNCLASSIFIED

EUGENE DIETZGEN CO.
MADE IN U. S. A.
LOGARITHMIC
CYCLES X 3 CYCLES

~~SECRET~~ UNCLASSIFIED

Perturbation Flux
Amplitude Ratio vs.
Specified Average Flux

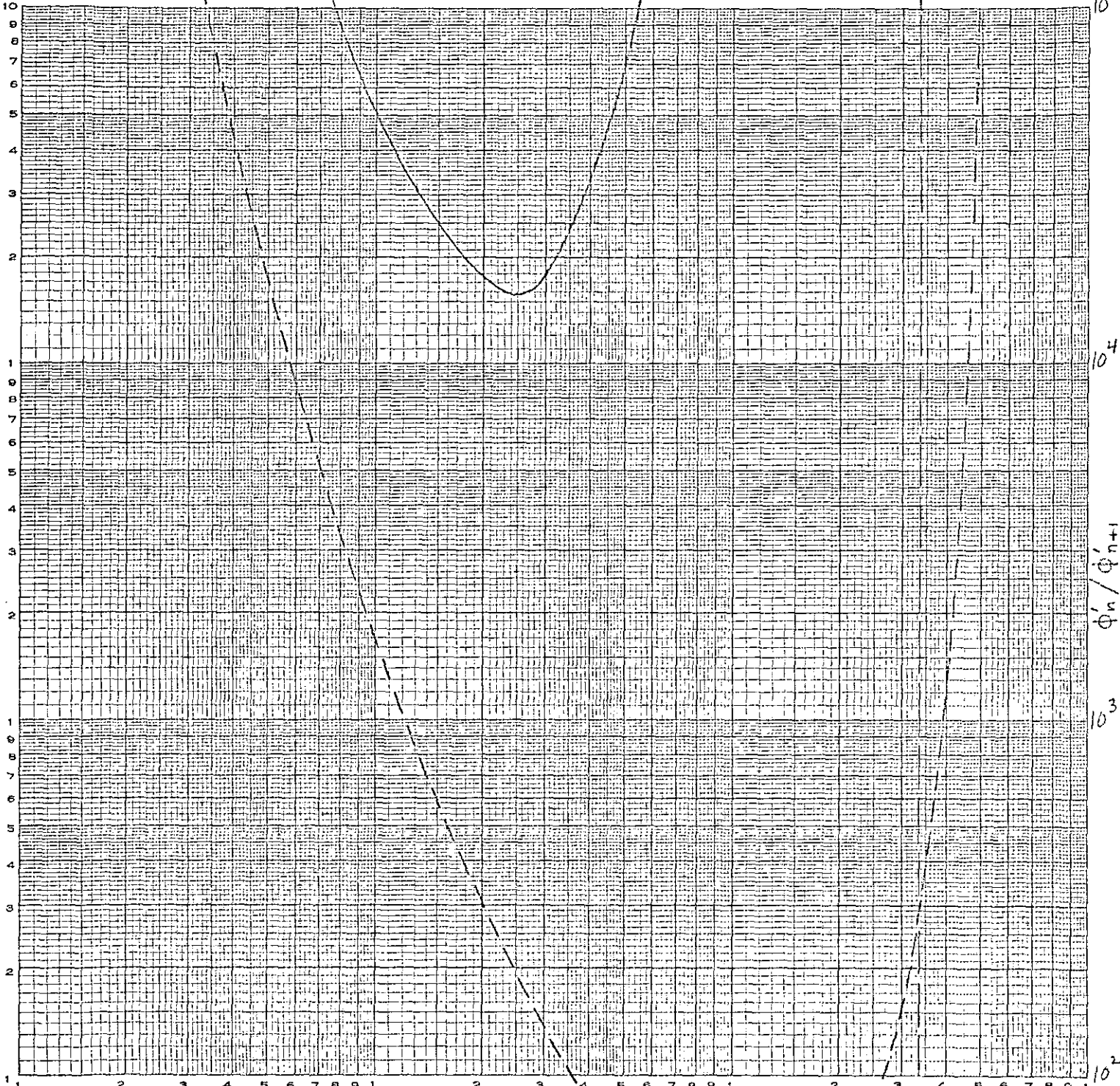
Figure 13.
DPST-68-206

-32-

0.50 flat

unflattened

operating flux



Axial Mode: Height = 381 cm.
 End of Cycle: $M^2 = 317 \text{ cm}^2$
 Temperature Coefficient = $-1.63 \times 10^{-17} \text{ k}/\phi$

No threshold
flux in either
case.

~~SECRET~~ UNCLASSIFIED

MADE IN U. S. A.

3 CYCLES X 3 CYCLES

UNCLASSIFIED

~~SECRET~~

P. L. ROGGENKAMP

-33-

DPST-68-206

to yielding a pair of thresholds; all four curves correspond to the "no threshold" case of Figure 7. In particular, the closest approach shown to threshold occurs at the start of the cycle: when the flux is 50% flattened, the amplitude ratio becomes as small as 3.5 at very nearly the actual flux level. Not shown is the somewhat more realistic 80% flat case (not calculated in sufficient detail), for which the ϕ'_n/ϕ'_{n+1} curves would cross the 1.0 line twice when the specified average flux = the threshold fluxes = 5.36×10^{13} and 7.84×10^{14} n/cm² sec. (Table I line 5); this would correspond to the "double threshold" case of Figure 7 (Figure 20 shows this situation for radial oscillation).

Figure 14 shows oscillation periods vs. flux levels for radial oscillations at the start of the cycle, if the temperature coefficient were zero. Single threshold fluxes exist for both unflattened and 50% flattened fluxes, cf. Figure 3. At the average operating flux level, any flux tilt perturbation superimposed on a 50% flat fundamental would grow in an oscillatory fashion with a period of 21 hours; such a flux tilt superimposed on a Jo fundamental would decay in an oscillatory manner with a period of 14 hours. At the end of the cycle, Figure 15, the Jo threshold flux has vanished and the 50% flat threshold has moved to a high flux level, cf. Figure 4. At the operating flux level, any flux tilt superimposed on a Jo fundamental would decay with a period of 15 hours; a flux tilt superimposed on a 50% flat fundamental would grow with a period of 11 hours.

Amplitude ratio curves for radial oscillation are shown for the hypothetical $\alpha_T = 0$ case because they illustrate the "single threshold" case of Figure 7. At the start of the cycle, Figure 16, each ϕ'_n/ϕ'_{n+1} curve crosses the 1.0 line once, corresponding to single thresholds at zero and 50% flatness. The 50% flat curve crosses the 1.0 line below the operating flux, indicating possible oscillations; the zero flat curve crosses the 1.0 line above the operating flux, so that divergent oscillations are impossible at the actual flux level. Note that the 50% flat curve yields an amplitude ratio of only 0.001 at the operating flux level, so that the perturbation amplitude for this hypothetical case would increase very rapidly if not countered by control rod adjustment.

At the end of the cycle, Figure 17, oscillations are possible when the flux is 50% flattened ("single threshold" case of Figure 7) because the amplitude ratio = 1.0 at a flux less than the operating flux, whereas oscillations are not possible when the flux is unflattened ("no threshold" case of Figure 7).

~~SECRET~~

UNCLASSIFIED

~~SECRET~~
-34-

increases steadily for $\phi \geq 2.297 \times 10^{17}$

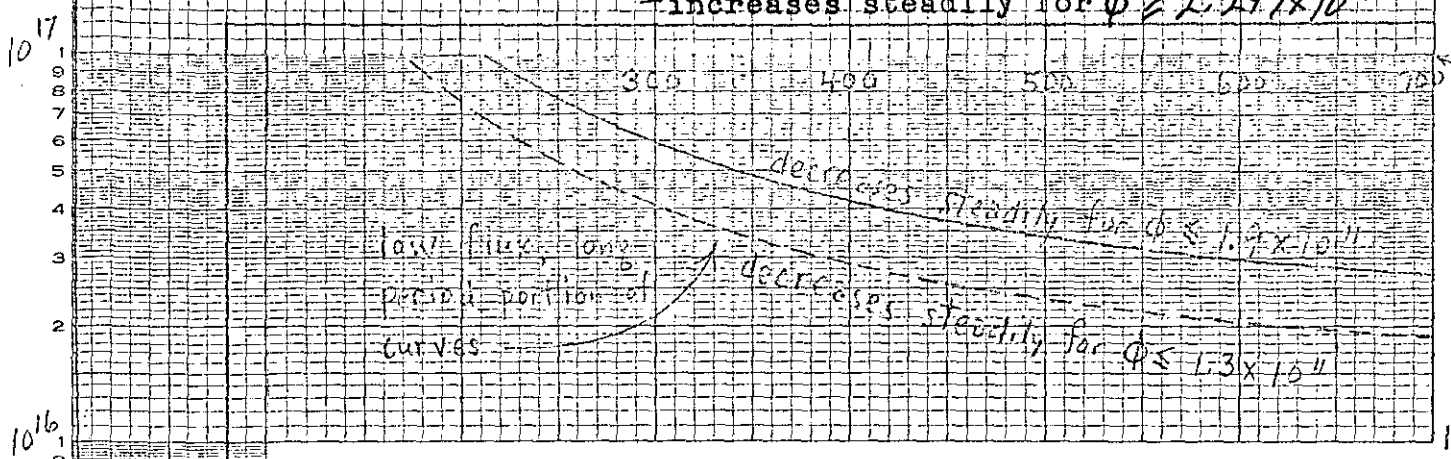


Figure 17

Oscillation Period for Any Given Flux Level

threshold flux = 1.98×10^{15} (unflattened)

increases steadily for $\phi \geq 2.2 \times 10^{17}$

operating flux

threshold flux = 5.89×10^{13} (0.50 flat)

Radial Mode: $r_{rad} = 25.6$ cm.
 Start of Cycle: $M^2 = 260$ cm².
 Temperature Coefficient = 0

unflattened

0.50 flat

Oscillation Period, hours

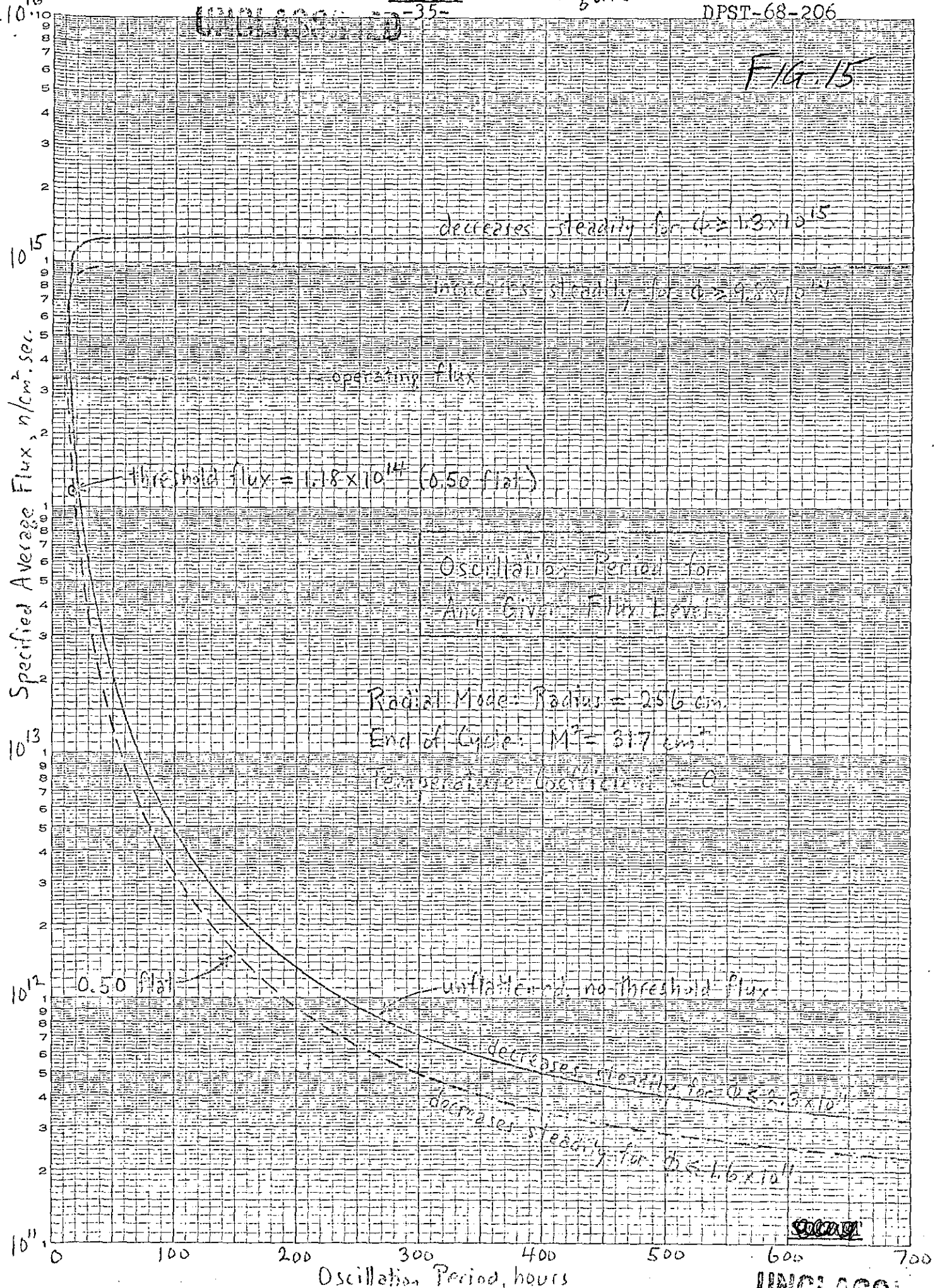
~~SECRET~~ UNCLASSIFIED

MADE IN U.S.A.

5 CYCLES X 10 DIVISIONS PER INCH

5 CYCLES X 10 DIVISIONS PER INCH

F16r.15



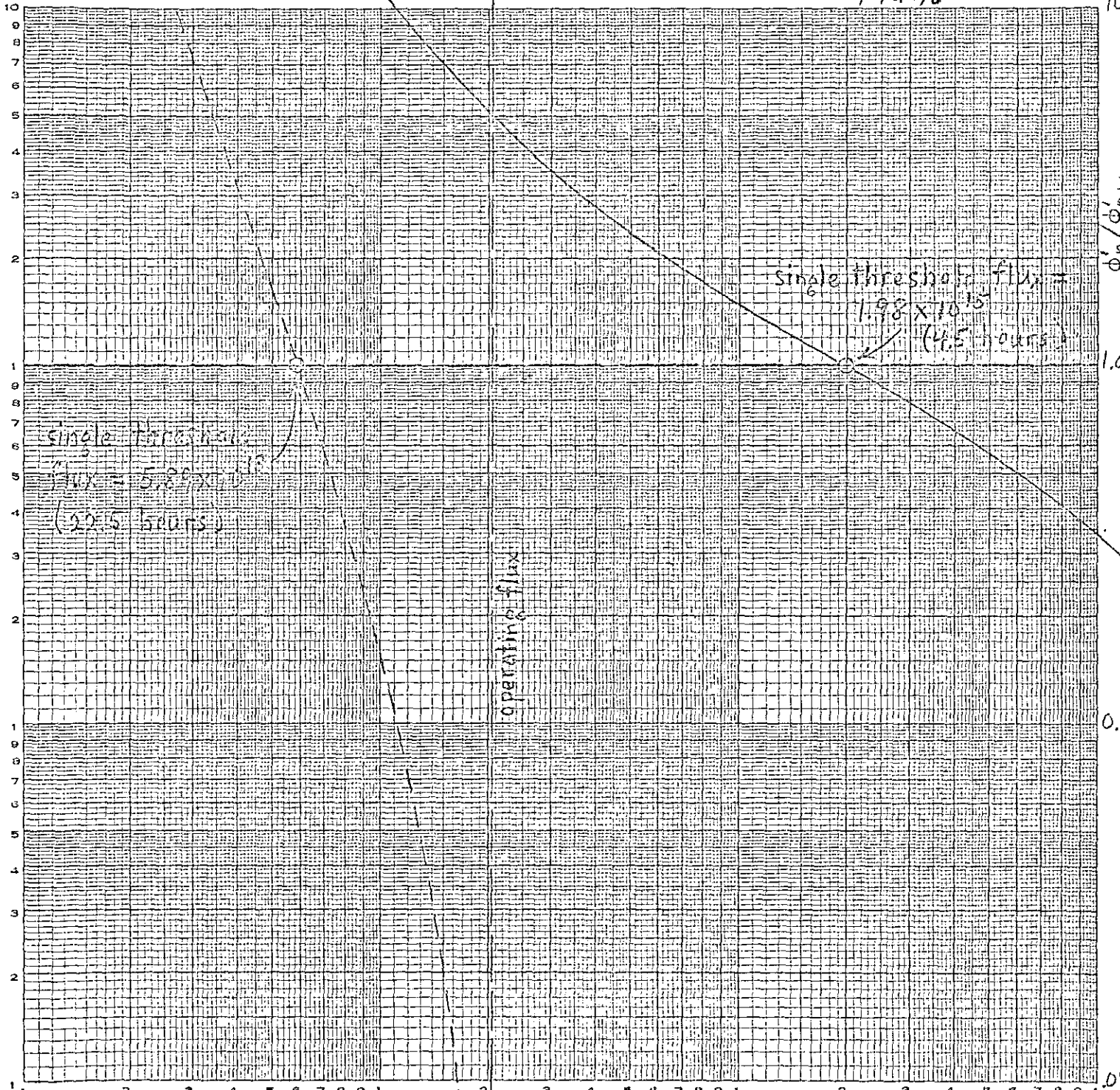
Oscillation Period, hours

UNCLASS

Figure 16.

Perturbation Flux Amplitude Ratio vs. Specified Average Flux

DPST-68-206
FIG. 16



EUGENE DIETZGEN CO.
MADE IN U.S.A.

LOGARITHMIC
1 3 CYCLES X 3 CYCLES

10^{13} $\Phi, n/cm^2 \cdot sec.$ 10^{14} 10^{15} 10^{16}

Radial Mode: Radius = 256 cm.
Start of Cycle: $M^2 = 260 \text{ cm}^2$
Temperature Coefficient = 0

~~SECRET~~
UNCLASSIFIED

Figure 17.

Perturbation Flux
Amplitude Ratio vs.
Specified Average Flux

~~SECRET~~
UNCLASSIFIED
-37-

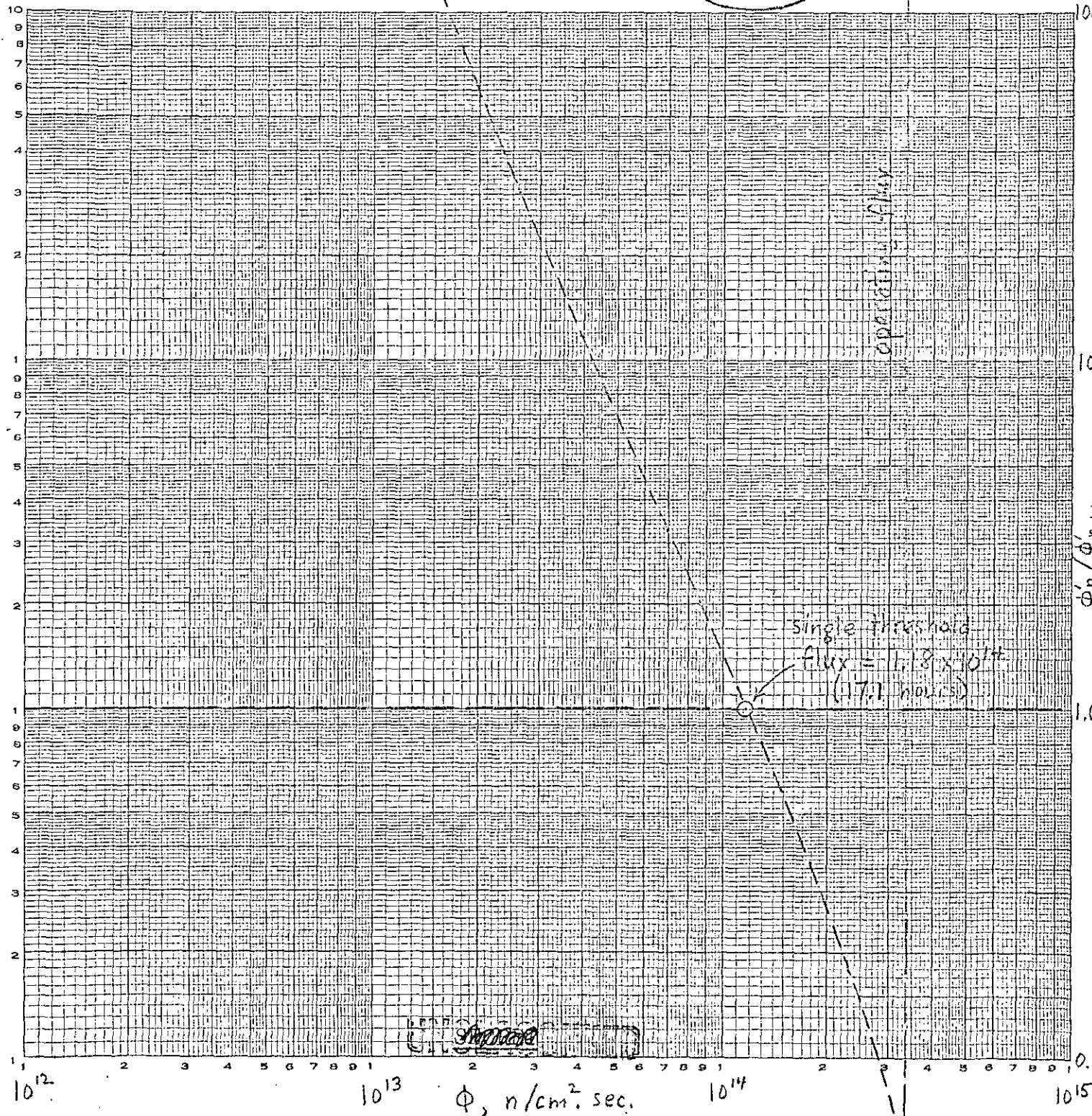
unflattened, no
threshold flux

DPST-68-206

FIG. 17

0.50 flat

EUGENE DIETZGEN CO.
MADE IN U. S. A.
LOGARITHMIC
3 CYCLES X 3 CYCLES



Radial Mode: Radius = 256 cm.
End of Cycle: $M^2 = 317 \text{ cm}^2$
Temperature Coefficient = 0

Figures 18 and 19 show similar curves for radial oscillations except that now $\alpha_T = -2.50 \times 10^{-17} \text{ k}/\phi$, its expected value. At the start of the cycle, Figure 18, the negative temperature coefficient has eliminated the Jo threshold present when $\alpha_T = 0$ (cf. Figure 14); the 50% flat threshold has now been replaced by a pair of thresholds (cf. Figure 3), the lower threshold of which ($7.33 \times 10^{13} \text{ n/cm}^2 \text{ sec.}$) lies somewhat above the single $\alpha_T = 0$ threshold ($5.89 \times 10^{13} \text{ n/cm}^2 \text{ sec.}$). This means that seven modes of behavior are possible for a 50% flat fundamental:

- (a) steady decay for $\phi \leq 1.3 \times 10^{11} \text{ n/cm}^2 \text{ sec.}$
- (b) oscillatory decay for $1.3 \times 10^{11} < \phi < \text{lower } \phi_{th} = 7.33 \times 10^{13} \text{ n/cm}^2 \text{ sec.}$
- (c) steady oscillation at $\phi = \text{lower } \phi_{th} = 7.33 \times 10^{13} \text{ n/cm}^2 \text{ sec.}$
- (d) oscillatory growth for $\text{lower } \phi_{th} = 7.33 \times 10^{13} < \phi < \text{upper } \phi_{th} = 3.95 \times 10^{14} \text{ n/cm}^2 \text{ sec.}$
- (e) steady oscillation at $\phi = \text{upper } \phi_{th} = 3.95 \times 10^{14} \text{ n/cm}^2 \text{ sec.}$
- (f) oscillatory decay for $\text{upper } \phi_{th} = 3.95 \times 10^{14} < \phi < 8.6 \times 10^{14} \text{ n/cm}^2 \text{ sec.}$
- (g) steady decay for $\phi \geq 8.6 \times 10^{14} \text{ n/cm}^2 \text{ sec.}$

In contrast, only three possibilities exist for the Jo fundamental:

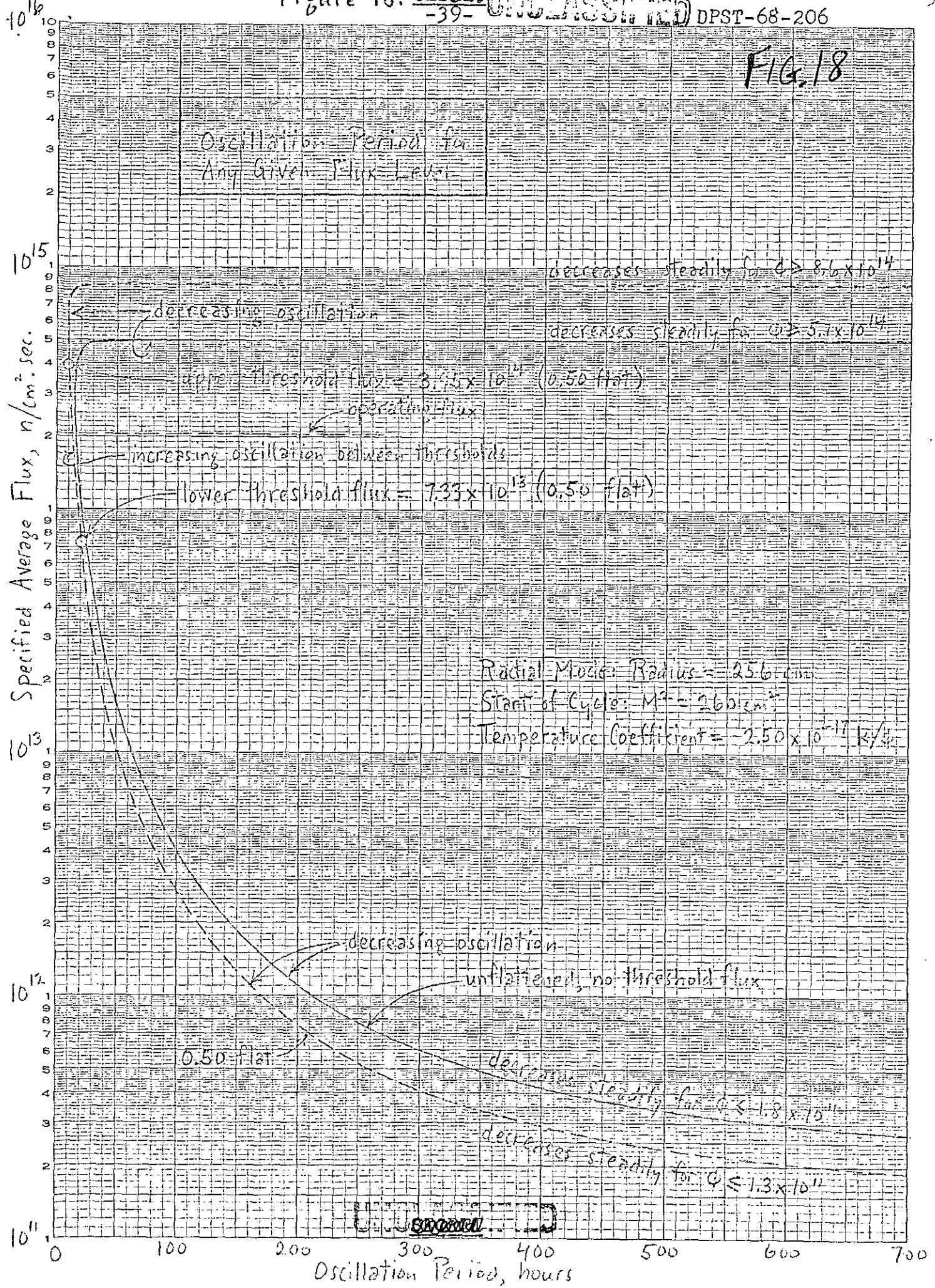
- (a) steady decay for $\phi \leq 1.8 \times 10^{11} \text{ n/cm}^2 \text{ sec.}$
- (b) oscillatory decay for $1.8 \times 10^{11} < \phi < 5.1 \times 10^{14} \text{ n/cm}^2 \text{ sec.}$
- (c) steady decay for $\phi \geq 5.1 \times 10^{14} \text{ n/cm}^2 \text{ sec.}$

At the initial average operating flux, any flux tilt perturbation superimposed on a Jo fundamental will decay with a period of 16 hours; such a perturbation imposed on a 50% flat fundamental will grow with a period of 14 hours.

At the end of the cycle, Figure 19, there is no threshold for either a Jo fundamental (also the case when $\alpha_T = 0$) or for a 50% flat fundamental (where a threshold does exist if $\alpha_T = 0$), cf. Figure 4. Thus all flux tilt perturbations will die out spontaneously; at the average operating flux, such a perturbation will decay steadily for a Jo fundamental or with a period of 12 hours for a 50% flat fundamental.

Amplitude ratio curves for radial oscillations are shown for the realistic negative α_T case in Figures 20 and 21. At the start of the cycle, two thresholds ($\phi'_n/\phi'_{n+1} = 1.0$) bracket the operating flux when the flux is 50% flattened, so that divergent oscillations can occur. At the operating flux level, $\phi'_n/\phi'_{n+1} = 0.25$ so that each successive perturbation peak is four times higher than the preceding peak. No threshold exists if the flux is unflattened (all $\phi'_n/\phi'_{n+1} > 1.0$).

FIG. 18



EUGENE DIETZEN CO.
MADE IN U. S. A.

NO. 340-LS10 DIETZEN GRAPH PAPER
SEMI-LOGARITHMIC
5 CYCLES X 10 DIVISIONS PER INCH

~~SECRET~~ UNCLASSIFIED

FIG. 19

Oscillation Period for Any Given Flux Level

EUGENE DIETZGEN CO. MADE IN U. S. A.

NO. 340 - LS10 DIETZGEN GRAPH PAPER SEMI-LOGARITHMIC 5 CYCLES X 10 DIVISIONS PER INCH

Specified Average Flux, $n/cm^2 \cdot sec.$

Oscillation Period, hours

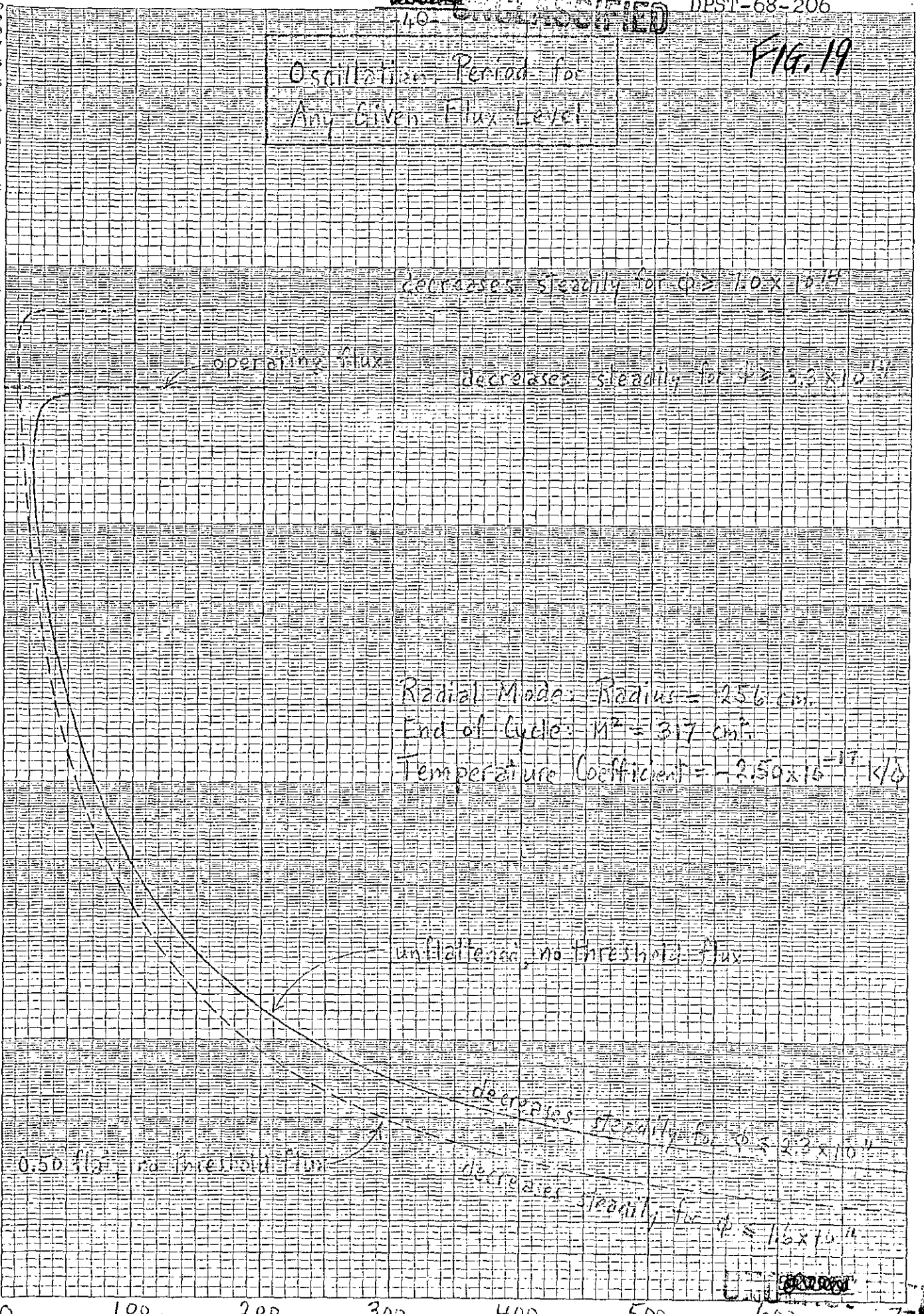


Figure 20.

Perturbation Flux
Amplitude Ratio vs.
Specified Average Flux

~~SECRET~~ UNCLASSIFIED

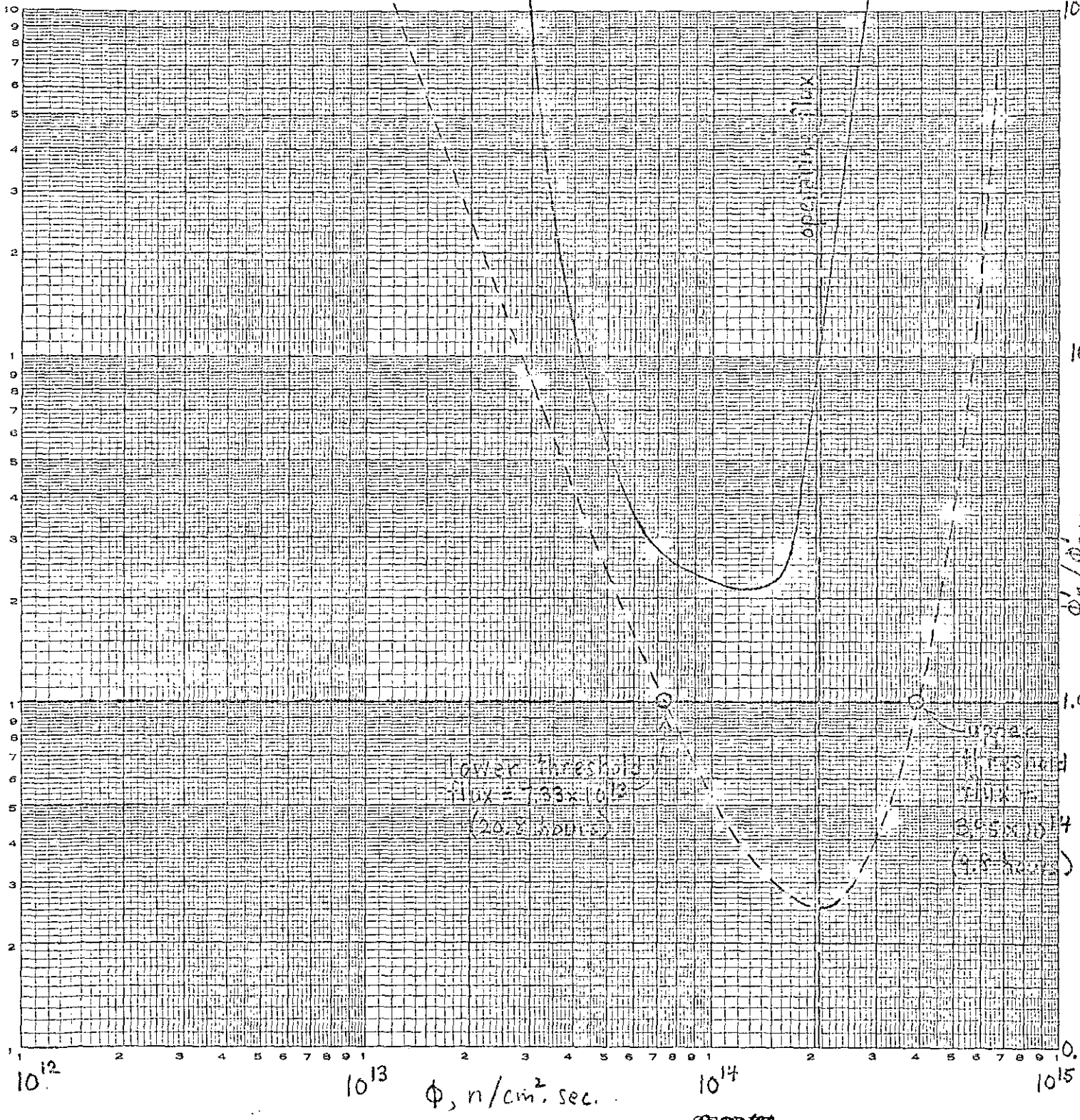
0.50 flat

unflattened, no
threshold flux

FIG. 20

EUGENE DIETZGEN CO.
MADE IN U. S. A.

LOGARITHMIC
3 CYCLES X 3 CYCLES



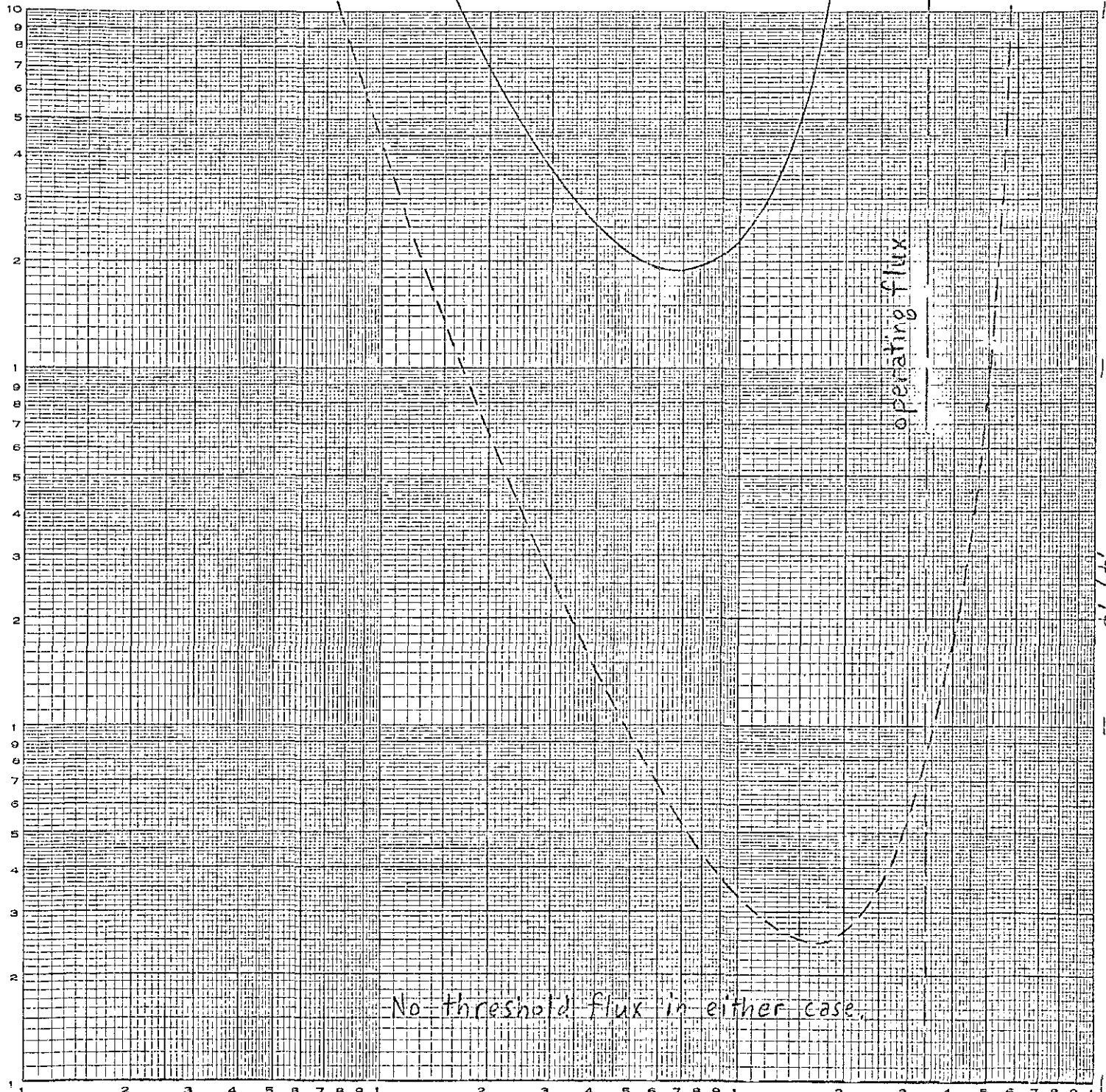
Radial Mode: Radius = 256 cm.
Start of Cycle: $M^2 = 260 \text{ cm}^2$
Temperature Coefficient = $-2.50 \times 10^{-17} \text{ k}/\phi$

~~SECRET~~ UNCLASSIFIED

unflattened UNCLASSIFIED

Perturbation Flux Amplitude Ratio vs. Specified Average Flux

0.50 flat



Radial Mode: Radius = 256 cm.
 End of Cycle: $M^2 = 317 cm^2$
 Temperature Coefficient = $-2.50 \times 10^{-17} k/\phi$

~~SECRET~~
 UNCLASSIFIED

EUGENE DIETZGEN CO.
 MADE IN U.S.A.

NO. 3441-L33 DIETZGEN GRAPH PAPER
 LOGARITHMIC
 3 CYCLES X 3 CYCLES

At the end of the cycle, no thresholds exist, so that only damped oscillations are possible. At the actual flux level, the amplitude ratio for 50% flattening is 8.4, so that each successive perturbation peak is only 12% as high as the preceding peak; and if the flux is unflattened, not even such convergent oscillations are possible at the operating level, because the amplitude ratio goes to infinity at a flux level just less than the operating flux.

IV. Effect of Changes in Input Parameters

The decay constants λ_I, λ_x and the fractional fission yields γ_I, γ_x were assigned the values shown on page 4 throughout this study. There was, however, some question as to what value to use for σ_x (cf. footnote p. 22) and especially for SIGRAT.

It was decided to use the HAMMER average value $\sigma_x = 2.60 \times 10^{-18}$ cm². Some preliminary calculations, listed in Table IV, show that using a higher 2200 m./sec. $\sigma_x = 3.08 \times 10^{-18}$ cm² would have resulted in somewhat lower calculated oscillation thresholds (compare lines 4 vs. 2, 7 vs. 5, 8 vs. 6), i.e., the reactor would have appeared to be less stable. Increasing σ_x lowers the threshold flux vs. threshold oscillation period curve, as shown in Figure 5.

Table IV

Effect of Changes in σ_x and SIGRAT

$$\alpha_T = 0, M^2 = 260 \text{ cm}^2$$

Mode	Fraction Flat	$10^{18} \sigma_x$ (cm ²) ^x	Threshold Flux at SIGRAT =		
			0.407	0.611	0.737
Axial	0	2.60	none	none	none
"	0.50	2.60	none	1.86×10^{14}	7.66×10^{13}
"	0	3.08	not run	none	none
"	0.50	3.08	not run	1.57×10^{14}	6.46×10^{13}
Radial	0	2.60	none	1.98×10^{15}	1.31×10^{14}
"	0.50	2.60	2.05×10^{15}	5.98×10^{13}	3.86×10^{13}
"	0	3.08	not run	1.67×10^{15}	1.10×10^{14}
"	0.50	3.08	not run	4.98×10^{13}	3.26×10^{13}

UNCLASSIFIED

~~SECRET~~

P. L. ROGGENKAMP

-44-

DPST-68-206

Columns 4, 5, and 6 of Table IV show that larger values of Sigrat yield significantly lower calculated oscillation thresholds. Column 6 lists the too-low threshold fluxes which would have been predicted if the lattice were regarded as homogeneous or uniformly loaded, page 6. This simplest approach would have underestimated the stability of the reactor. Column 4 lists the too-high thresholds which would have been predicted if the lattice were regarded as heterogeneous (mixed lattice) without taking the enhancement effect into account, page 7. This approach would have been non-conservative in that, for the conditions tested, no xenon oscillations at all would have been predicted: the single flux threshold shown lies above the operating average flux. Column 5 lists the most realistic thresholds, taking into account both heterogeneity and enhancement, page 8.

UNCLASSIFIED

UNCLASSIFIED

~~SECRET~~

-45-

P. L. ROGGENKAMP

DPST-68-206

References

1. D. Randall, D. S. St. John, Xenon Spatial Oscillations, Nucleonics 16, 82 (March 1958).
2. D. Randall, D. S. St. John, Xenon Spatial Oscillations, Nuclear Science and Engineering 14, 204, (October, 1962).
3. DPSTM-XIIA(P). Technical Manual, Physics of Mark XIIA and Mark 50 Assemblies, June, 1967.
4. DP report to be published.
5. D. Randall, Xenon Stability in New Production Charges, DPST-65-261, May 3, 1965.
6. M. D. Goldberg, et al., Neutron Cross Sections, BNL-325, Second Edition, Supplement No. 2, Volume IIB, Z = 41 to 60. Sigma Center, Brookhaven National Laboratory, Associated Universities, Inc., May, 1966.

~~SECRET~~

UNCLASSIFIED